

Supporting Information

Tuning photochemical properties of phosphorus(V) porphyrins photosensitizers

Ivan N. Meshkov^{a,b}, Véronique Bulach^a, Yulia G. Gorbunova^{b,c*}, Fedor E. Gostev,^d Victor A. Nadtochenko,^d Aslan Yu. Tsivadze^{b,c}, and Mir Wais Hosseini^a

^aMolecular Tectonics Laboratory, UMR UDS-CNRS, 7140 & icFRC, Université de Strasbourg, F-67000, Strasbourg, France

^bFrumkin Institute of Physical Chemistry and Electrochemistry, Russian Academy of Sciences, Leninsky pr. 31-4, Moscow, 119071 Russia

^cKurnakov Institute of General and Inorganic Chemistry, Russian Academy of Sciences, Leninsky pr. 31, Moscow, 119991 Russia

^dSemenov Institute of Chemical Physics, Russian Academy of Sciences, Kosygina st. 4, Moscow, 119991 Russia
e-mail: yulia@igic.ras.ru, hosseini@unistra.fr

Experimental section		Page S3
Figure S1	Experimental setups for SO measurements in organic (left) and aqueous (right) media.	Page S8
Table 1	Stokes shifts and emission maxima of P(V) porphyrins.	Page S11
Table 2	Quantum yields of S ₁ -S ₀ , S ₁ -CT and S ₁ -T ₁ processes calculated from transient absorption experiments.	Page S11
Scheme 1	Jablonski diagram of energy transitions in photosensitive porphyrin.	Page S12
Figure S2	¹ H-NMR (bottom, CDCl ₃ , 300 MHz, 25 °C) and ³¹ P-NMR (top right, CDCl ₃ , 121 MHz, 25 °C) spectra of 2a .	Page S13
Figure S3	HR-ESI TOF spectrum of 2a .	Page S13
Figure S4	¹ H-NMR (bottom, CDCl ₃ , 400 MHz, 25 °C) and ³¹ P-NMR (top right, CDCl ₃ , 162 MHz, 25 °C) spectra of 3a .	Page S14
Figure S5	HR-ESI TOF spectrum of the compound 3a .	Page S14
Figure S6	¹ H-NMR (bottom, CDCl ₃ , 500 MHz, 25 °C) and ³¹ P-NMR (top right, CDCl ₃ , 121 MHz, 25 °C) spectra of 4a .	Page S15
Figure S7	HR-ESI TOF spectrum of the compound 4a .	Page S15
Figure S8	¹ H NMR (bottom, CDCl ₃ , 300 MHz, 25 °C) and ³¹ P NMR (top right, CDCl ₃ , 162 MHz, 25 °C) spectra of the compound 5a .	Page S16
Figure S9	HR-ESI TOF spectrum of the compound 5a .	Page S16
Figure S10	¹ H-NMR (bottom, CDCl ₃ , 300 MHz, 25 °C) and ³¹ P-NMR (top right, CDCl ₃ , 121 MHz, 25 °C) spectra of 2b .	Page S17
Figure S11	HR-ESI TOF spectrum of the compound 2b .	Page S17
Figure S12	¹ H-NMR (bottom, CDCl ₃ , 400 MHz, 25 °C) and ³¹ P-NMR (top right, CDCl ₃ , 162 MHz, 25 °C) spectra of 3b .	Page S18
Figure S13	HR-ESI TOF spectrum of the compound 3b .	Page S18
Figure S14	¹ H-NMR (bottom, CDCl ₃ , 400 MHz, 25 °C) and ³¹ P-NMR (top right, CDCl ₃ , 162 MHz, 25 °C) spectra of 4b .	Page S19
Figure S15	HR-ESI TOF spectrum of the compound 4b .	Page S19
Figure S16	¹ H NMR (bottom, CDCl ₃ +DMSO _{d6} , 300 MHz, 25 °C) and ³¹ P NMR	Page S20

	(top right, CDCl ₃ +DMSO _{d6} , 162 MHz, 25 °C) spectra of the compound 5b .	
Figure S17	HR-ESI TOF spectrum of the compound 5b .	Page S20
Figure S18	Normalized UV-Vis spectra of compounds 2a-5a in CHCl ₃ .	Page S21
Figure S19	Normalized UV-Vis spectra of compounds 2b-5b in CHCl ₃ .	Page S21
Figure S20	Normalized UV-Vis spectra of compounds 2a-5a in DMSO.	Page S22
Figure S21	Normalized UV-Vis spectra of compounds 2b-5b in DMSO.	Page S22
Figure S22	Normalized UV-Vis spectra of compounds 3a-5a in water.	Page S23
Figure S23	Normalized UV-Vis spectra of compounds 3b-5b in water.	Page S23
Figure S24	Normalized fluorescence spectra ($\lambda_{\text{ex}} = 550 \text{ nm}$) of compounds 2a-5a in CHCl ₃ .	Page S24
Figure S25	Normalized fluorescence spectra ($\lambda_{\text{ex}} = 550 \text{ nm}$) of compounds 2b-5b in CHCl ₃ .	Page S24
Figure S26	Normalized fluorescence spectra ($\lambda_{\text{ex}} = 550 \text{ nm}$) of compounds 2a-5a in DMSO.	Page S25
Figure S27	Normalized fluorescence spectra ($\lambda_{\text{ex}} = 550 \text{ nm}$) of compounds 2b-5b in DMSO.	Page S25
Figure S28	Normalized fluorescence spectra ($\lambda_{\text{ex}} = 550 \text{ nm}$) of compounds 3a-5a in water.	Page S26
Figure S29	Normalized fluorescence spectra ($\lambda_{\text{ex}} = 550 \text{ nm}$) of compounds 3b-5b in water.	Page S26
Figure S30	Degradation of DPBF in the chloroform solution of 2a .	Page S27
Figure S31	Degradation of DPBF in the chloroform solution of 2a – plot of DPBF peak (415 nm) vs time	Page S27
Figure S32	Transient spectra at early time delays of 2a, 4a, 5a	Page S28
Figure S33	2D maps of transient spectra changes vs time delay.	Page S29
Figure S34	Transient spectra in the region of the Soret band vs time delay of 2a, 4a, 5a	Page S30
Figure S35	Transient absorption spectra of complexes 4a and 5a	Page S31
	Intramolecular energy transitions without CT state for compounds 2, 3 and 5 .	Page S32
	Intramolecular energy transitions with CT state for compounds 4 .	Page S33
	Calculated transient absorption spectra data for complexes 2-5 .	Page S34
Figure S36	Calculated molecular orbitals of 2a .	Page S35
Figure S37	Calculated molecular orbitals of 3a .	Page S35
Figure S38	Calculated molecular orbitals of 4a .	Page S35
Figure S39	Calculated molecular orbitals of 5a .	Page S35
Figure S40	Calculated molecular orbitals of 2b	Page S36
Figure S41	Calculated molecular orbitals of 3b	Page S36
Figure S42	Calculated molecular orbitals of 4b	Page S36
Figure S43	Calculated molecular orbitals of 5b	Page S36
References		Page S37

Experimental section

General procedures. Solvents were dried using standard techniques: CH₂Cl₂ and CHCl₃ were distilled over CaH₂. All air and water sensitive experiments were carried out under argon atmosphere using standard vacuum line techniques. All chemicals were obtained commercially and used without further purification, except pyrrole which was purified over an alumina column before use.

¹H, ¹³C and ³¹P NMR spectra were acquired on either a Bruker AV 300 (300MHz), a Bruker AV 400 (400 MHz) or a Bruker AV 500 (500 MHz) spectrometer, with a deuterated solvent as the lock and residual solvent as the internal reference. Absorption spectra were recorded using either a Lambda 650S spectrophotometer (PerkinElmer) or an Evolution 210 spectrophotometer (Thermo Scientific). A MicroTOF-Q LC (Bruker Daltonics, Bremen) spectrometer equipped with an electrospray source was used for the high-resolution electrospray mass spectrometry measurements (HR ESI-MS). BioRad Bio Beads S-X1 and S-X3 gels were used for the gel-permeation chromatography (GPC).

Synthesis. Here, only the synthetic procedures for the preparation of the P(V) complexes **2a-5a** and **2b-5b** are given. Free-base porphyrins **1a-1b** were prepared following previously described procedure.¹

Compound 2a was obtained according to a modified literature procedure². The free-base porphyrin **1a** (0.1 g, 0.16 mmol, 1 equiv) was dissolved in 18 ml of pyridine under argon and POCl₃ (2 ml, 21.96 mmol, 135 equiv) was added dropwise to the mixture under stirring. A solution of PCl₅ (0.1 g, 0.48 mmol, 3 equiv) in 2 ml of pyridine was then added dropwise and the mixture was refluxed under argon during 24 h. After cooling to the room temperature and evaporation of pyridine under vacuum, the dark green solid was dissolved in 50 ml of CH₂Cl₂ and washed with distilled water (3 x 400 ml) to remove residual pyridine. The organic layer was isolated and after evaporation of CH₂Cl₂, the green solid was purified by column chromatography on alumina using CH₂Cl₂-methanol (95:5) as eluent. The major main fraction was isolated and evaporated to dryness before it was further purified by chromatography on BioBeads S-X3 column (eluent – chloroform) affording 0.1 g (yield 82%) of pure compound **2a** as a green solid. ¹H NMR (CDCl₃, 300 MHz): δ 7.80 (m, 12H, CH_{Ph meta/para}), 7.99 (m, 8H, CH_{Ph ortho}), 9.14 (d, ⁴J_{P-H} = 4.5 Hz, 8H, CH_{β-pyrrolic}). ³¹P NMR (CDCl₃, 121 MHz): δ -229. ¹³C NMR (CDCl₃, 125 MHz): δ 117.7 (C, ³J_{P-C} = 3.3 Hz), 128.8 (CH), 130.5 (CH), 132.8 (CH, ³J_{P-C} = 6.5 Hz),

133.3 (CH), 134.2 (C), 140.0 (C). UV-Vis (CHCl₃) λ max (nm) (log ϵ , mol⁻¹ L cm⁻¹) 440 (5.44), 568 (4.13), 613 (4.00). HR-ESI MS: m/z obsd 713.1407, calcd 713.1423 [(M-Cl)⁺; M = C₄₄H₂₈Cl₃N₄P].

Compound 3a. The porphyrin **1a** (0.1 g, 0.16 mmol, 1 equiv) was dissolved in pyridine (60 ml) under argon and POBr₃ (1.1 g, 4.06 mmol, 25 equiv) previously dissolved in pyridine (20 ml) was added dropwise to the mixture under stirring. The reaction mixture was refluxed during 80 min under argon and then cooled to room temperature. The green mixture was then poured into 150 ml of CH₂Cl₂ and 2L of distilled water was added and the mixture stirred during 2 days at room temperature until full hydrolysis of [P(TPP)(Br)₂]Br to the dihydroxy complex [P(TPP)(OH)₂]⁺Br⁻ was completed. The organic layer was isolated and diluted with petroleum ether (150 ml). The mixture was poured directly on a SiO₂ chromatography column without evaporation of solvents. Increasing the polarity of the eluent using CH₂Cl₂-MeOH mixture (90:10) gives the crude product. Further purification of product by Bio-Beads S-X1 GPC (eluent – chloroform-methanol 98:2) afforded 0.115 g of the pure purple compound **3a** in 95 % yield. ¹H NMR (CDCl₃, 400 MHz): δ 7.69 (m, 12H, CH_{Ph meta/para}), 8.01 (m, 8H, CH_{Ph ortho}), 8.89 (d, ⁴J_{P-H} = 2.7 Hz, 8H, CH _{β -pyrrolic}). ³¹P NMR (CDCl₃, 162 MHz): δ -193. ¹³C NMR (CDCl₃, 125 MHz): δ 115.9 (C), 127.7 (CH), 128.7 (CH), 132.0 (CH), 133.7 (CH), 134.7 (C), 139.5 (C). UV-Vis (CHCl₃) λ max (nm) (log ϵ , mol⁻¹ L cm⁻¹) 428 (5.42), 556 (4.21), 596 (3.92). HR-ESI MS: m/z obsd 677.2084, calcd 677.2101 [(M-Br)⁺, M = C₄₄H₃₀BrN₄O₂P].

Compound 4a. The complex **2a** (0.04 g, 0.053 mmol, 1 equiv) was dissolved in pyridine (10 ml) then 3-methoxyphenol (17 μ l, 0.155 mmol, 3 equiv) previously dissolved in 5 ml of pyridine was added dropwise. The reaction mixture was refluxed overnight under argon. Pyridine was removed under vacuum and the solid residue was purified by column chromatography on alumina using a mixture of methanol-CH₂Cl₂ as an eluent (from 0% to 10% of MeOH). Further purification by Bio-Beads S-X1 GPC (eluent - chloroform-methanol 98:2) afforded 24 mg of the pure green product **4a** (50% yield). ¹H NMR (CDCl₃, 500 MHz): δ 1.25 (br., 2H, CH_{Res}), 1.80 (d, ³J = 8.2 Hz, 2H, CH_{Res}), 3.11 (s, 6H, CH₃), 5.68 (d, ³J = 8.3 Hz, 2H, CH_{Res}), 5.84 (dd, ³J = 8.2 Hz, ³J = 8.2 Hz, 2H, CH_{Res}), 7.76 (m, 20H, CH_{Ph}), 9.04 (d, ⁴J_{P-H} = 2.7 Hz, 8H, CH _{β -pyrrolic}). ³¹P NMR (CDCl₃, 162 MHz): δ -196. ¹³C NMR (CDCl₃, 125 MHz): δ 54.9 (CH₃), 101.5 (CH, ³J_{P-C} = 8.8 Hz), 106.8 (CH, ³J_{P-C} = 8.6 Hz), 107.6 (CH), 117.2 (C), 128.4 (CH), 128.6 (CH), 130.1 (CH), 133.4 (CH, ³J_{P-C} = 6.1 Hz), 133.6 (CH), 134.9 (C), 139.6 (C), 150.1 (C, ²J_{P-C} = 17.4 Hz), 158.7

(C). UV-Vis (CHCl₃) λ max (nm) ($\log\epsilon$, mol⁻¹ L cm⁻¹) 435 (5.00), 565 (4.10), 606 (3.79). HR-ESI MS: m/z obsd 889.2944, calcd 889.2938 [(M-Cl)⁺]; M = C₅₈H₄₂ClN₄O₄P.

Compound 5a. The porphyrin **1a** (0.1 g, 0.16 mmol, 1 equiv) was dissolved in pyridine (60 ml) under argon and POBr₃ (1.1 g, 4.06 mmol, 25 equiv) previously dissolved in pyridine (20 ml) was added dropwise to the mixture under stirring. The reaction mixture was refluxed during 80 min under argon and then cooled to room temperature. The green mixture was then poured into 100 ml of ethanol and the obtained mixture stirred 2 days at room temperature until full transformation of the Br-intermediate into the target compound. The mixture was diluted with CH₂Cl₂ (200 ml) and washed with distilled water (3 x 500 ml) to remove pyridine and ethanol. The organic layer was isolated, diluted with 200 ml of petroleum ether and poured directly on a SiO₂ chromatography column without evaporation of solvents. Increasing the polarity of the eluent using CH₂Cl₂-MeOH mixture (90:10) gives the crude product. Further purification by Bio-Beads S-X1 GPC (eluent – CHCl₃-MeOH 98:2) afforded 84 mg of the pure purple compound **5a** in 64% yield. ¹H NMR (CDCl₃, 300 MHz): δ -2.34 (dq, ³J_{P-H} = 14.0 Hz, ³J = 7.0 Hz, 4H, CH₂), -1.79 (td, ³J = 7.3 Hz, ⁴J_{P-H} = 2.1 Hz, 6H, CH₃), 7.79 (m, 12H, CH_{Ph meta/para}), 7.95 (m, 8H, CH_{Ph ortho}), 9.07 (d, ⁴J_{P-H} = 2.7 Hz, 8H, CH _{β -pyrrolic}). ³¹P NMR (CDCl₃, 162 MHz): δ -179. ¹³C NMR (CDCl₃, 125 MHz): δ 13.1 (CH₃, ³J_{P-C} = 16.4 Hz), 56.9 (CH₂, ²J_{P-C} = 15.0 Hz), 115.4 (C, ³J_{P-C} = 2.0 Hz), 128.6 (CH), 129.9 (CH), 132.2 (CH, ³J_{P-C} = 5.0 Hz), 133.3 (CH), 135.4 (C), 139.2 (C). UV-Vis (CHCl₃) λ max (nm) ($\log\epsilon$, mol⁻¹ L cm⁻¹) 429 (5.44), 558 (4.23), 595 (4.02). HR-ESI MS: m/z obsd 733.2737, calcd 733.2727 [(M-Br)⁺], M = C₄₈H₃₈BrN₄O₂P.

Compound 2b. The porphyrin **1b** (0.1 g, 0.16 mmol, 1 equiv) was dissolved in pyridine (20 ml) and solutions of POCl₃ (2 ml, 21.93 mmol, 135 equiv) and PCl₅ (0.1 g, 0.49 mmol, 3 equiv) in 2 ml of pyridine were added dropwise under argon. The mixture was refluxed during 72 h under argon. The pyridine was evaporated under vacuum and the green residue was purified by column chromatography on alumina. Gradual addition of methanol up to 5% afforded the crude compound. After evaporation, the solid was further purified by Bio-Beads S-X1 GPC with chloroform as the eluent affording 48 mg (yield 40%) of compound **2b** as a green solid. **Method B.** The porphyrin **3b** (19 mg, 0.038 mmol, 1 equiv), (see below) was dissolved in chloroform (5 ml) under argon and SOCl₂ (2 ml, 27 mmol, 720 equiv) was added. The mixture was stirred during 12 h at room temperature and the solvent as well as excess of thionyl chloride were removed under vacuum. Chloroform (5 ml) was added and the mixture was passed through Bio-

Beads S-X1 GPC column with chloroform as eluent affording 19 mg (100% yield) of the compound **2b** as a green solid. ^1H NMR ($\text{CDCl}_3 + \text{DMSO-d}_6$, 300 MHz): δ 7.48 (m, 9H, CH_{Ph} meta/para), 7.63 (d, $^3J = 6.7$ Hz, 6H, CH_{Ph} ortho), 7.79 (m, 2H, CH_{Py} ortho), 8.78-8.88 (m, 10H, CH_{β} -pyrrolic/Py meta). ^{31}P NMR ($\text{CDCl}_3 + \text{DMSO-d}_6$, 121 MHz): δ -229. ^{13}C NMR ($\text{CDCl}_3 + \text{DMSO-d}_6$, 125 MHz): δ 111.5 (C), 118.4 (C, $^3J_{\text{P-C}} = 3.0$ Hz), 118.7 (C, $^3J_{\text{P-C}} = 3.0$ Hz), 127.7 (C), 128.1 (C), 128.9 (CH), 130.6 (CH, $^3J_{\text{P-C}} = 3.4$ Hz), 133.1 (CH, $^3J_{\text{P-C}} = 6.6$ Hz), 133.3 (CH, $^3J_{\text{P-C}} = 6.6$ Hz), 133.4 (CH), 133.5 (CH), 134.0 (CH), 134.1 (CH), 134.6 (CH, $^3J_{\text{P-C}} = 6.5$ Hz), 138.7 (C), 139.8 (C), 140.3 (C), 140.4 (C). UV-Vis (CHCl_3) λ max (nm) ($\log\epsilon$, $\text{mol}^{-1} \text{L cm}^{-1}$) 439 (5.32), 570 (4.02), 608 (3.81). HR-ESI MS: m/z obsd 714.1341, calcd 714.1376 [(M-Cl) $^+$; M = $\text{C}_{43}\text{H}_{27}\text{Cl}_3\text{N}_5\text{P}$].

Compound 3b. The porphyrin **1b** (63 mg, 0.1 mmol, 1 equiv) was dissolved in pyridine (30 ml) under argon and a solution of POBr_3 (1.17 g, 4.09 mmol, 40 equiv) in pyridine (20 ml) was added dropwise under stirring. The reaction mixture was refluxed during 1.5 h under argon and then cooled to room temperature. After adding CH_2Cl_2 (150 ml), to the green suspension 2 L of distilled water was added and the mixture stirred at room temperature during 1 day until full hydrolysis of $\text{P}(\text{MPyP})(\text{Br})_2]^+\text{Br}^-$ to the dihydroxy complex $[\text{P}(\text{MPyP})(\text{OH})_2]^+\text{Br}^-$ was completed. The organic layer was isolated and placed on a silica gel chromatography column without evaporation of CH_2Cl_2 . Increasing the methanol ratio in the eluent up to 15% give the crude product. Further purification by Bio-Beads S-X1 GPC (eluent - chloroform-methanol 98:2) afforded 65 mg (85% yield) of the pure purple compound **3b**. ^1H NMR (CDCl_3 , 400 MHz): δ - 3.85 (br., 2H, OH), 7.71 (m, 9H, CH_{Ph} meta/para), 7.95 (m, 2H, CH_{Py} ortho), 8.00 (m, 6H CH_{Ph} ortho), 8.68 (dd, $^3J = 5.1$ Hz, $^4J_{\text{P-H}} = 1.3$ Hz, 2H, CH_{β} -pyrrolic), 8.76 (d, $^4J_{\text{P-H}} = 1.3$ Hz, 4H, CH_{β} -pyrrolic), 8.78 (dd, $^3J = 5.1$ Hz, $^4J_{\text{P-H}} = 1.3$ Hz, 2H, CH_{β} -pyrrolic), 8.92 (m, 2H, CH_{Py} meta). ^{31}P NMR (CDCl_3 , 162 MHz): δ -193. ^{13}C NMR (CDCl_3 , 125 MHz): δ 111.8 (C), 116.2 (C), 116.4 (C), 126.9 (CH), 127.8 (CH), 128.3 (CH), 129.0 (CH), 129.5 (CH), 131.4 (CH), 132.4 (C), 132.5 (CH), 132.9 (CH), 133.6 (CH), 134.7 (CH), 138.3 (C), 139.4 (C), 139.5 (C), 147.6 (CH), 148.6 (CH). UV-Vis (CHCl_3) λ max (nm) ($\log\epsilon$, $\text{mol}^{-1} \text{L cm}^{-1}$) 428 (5.24), 556 (4.02), 598 (3.32). HR-ESI MS: m/z obsd 339.6031, calcd 339.6063 [(M+H-Br) $^{2+}$]; obsd 678.2036, calcd 678.2053 [(M-Br) $^+$]; M = $\text{C}_{43}\text{H}_{29}\text{BrN}_5\text{O}_2\text{P}$.

Compound 4b. The porphyrin **2b** (50 mg, 0.067 mmol, 1 equiv) was dissolved in pyridine (10 ml) and then a solution of 3-methoxyphenol (22 μl , 0.20 mmol, 3 equiv) in pyridine (5 ml)

was added dropwise. The reaction mixture was refluxed overnight under argon. Pyridine was removed under vacuum and the solid residue was purified by column chromatography on silica gel using methanol-CH₂Cl₂ mixture as the eluent (from 0% to 15% of MeOH). Further purification by Bio-Beads S-X1 GPC (eluent - chloroform-methanol 98:2) afforded 30 mg (yield 50%) of the compound **4b** as a green solid. ¹H NMR (CDCl₃, 400 MHz): δ 1.24 (br., 2H, CH_{Res}), 1.75 (br., 2H, CH_{Res}), 3.11 (s, 6H, CH₃), 5.68 (d, ³J = 8.0 Hz, 2H, CH_{Res}), 5.84 (dd, ³J = 8.0 Hz, ³J = 8.0 Hz, 2H, CH_{Res}), 7.69-7.81 (m, 17H, CH_{Ph}, CH_{Py ortho}), 9.06 (m, 8H, CH_{β-pyrrolic}), 9.12 (m, 2H, CH_{Py meta}). ³¹P NMR (CDCl₃, 162 MHz): δ -195. ¹³C NMR (CDCl₃, 125 MHz): δ 55.0 (CH₃), 101.7 (CH, ³J_{P-C} = 9.0 Hz), 106.8 (CH, ³J_{P-C} = 9.1 Hz), 107.6, (CH), 117.8 (C) 128.5 (CH), 128.6 (CH), 130.2 (CH), 132.7 (CH), 133.6 (CH), 133.8 (CH), 134.4 (CH), 134.7 (CH), 139.5 (C), 139.7 (C), 139.8 (C), 150.0 (C), 158.7 (C). UV-Vis (CHCl₃) λ max (nm) (logε, mol⁻¹ L cm⁻¹) 434 (5.00), 564 (4.00), 606 (3.61). HR-ESI MS: *m/z* obsd 445.6458, calcd 445.6482 [(M+H-Cl)²⁺]; obsd 890.2873, calcd 890.2891 [(M-Cl)⁺]; M = C₅₇H₄₁ClN₅O₄P.

Compound 5b. The porphyrin **1b** (95 mg, 0.15 mmol, 1 equiv) was dissolved in pyridine (30 ml) under argon and POBr₃ (1.77 g, 6.17 mmol, 40 eq.) previously dissolved in pyridine (20 ml) was added dropwise to the mixture under stirring. The reaction mixture was refluxed for 1,5 h under argon and then cooled to room temperature. The green mixture was then poured into 200 ml of ethanol and the obtained mixture stirred 1 day at room temperature until full transformation of the Br-intermediate into the target compound. The mixture was diluted with CH₂Cl₂ (500 ml) and washed with distilled water (5 x 500 ml) to remove pyridine and ethanol. The organic layer was isolated and poured on a SiO₂ chromatography column without evaporation of solvents. Increasing the polarity of the eluent using CH₂Cl₂-MeOH mixture (85:15) gives the crude product. Further purification by Bio-Beads S-X1 GPC (eluent - CHCl₃-MeOH 98:2) afforded 84 mg (yield 66%) of the pure purple compound **5b** in 66% yield. ¹H NMR (CDCl₃+DMSO_{d6}, 300 MHz): δ -2.35 (dq, ³J_{P-H} = 13.7 Hz, ³J = 7.3 Hz, 4H, CH₂), -1.74 (td, ³J = 7.0 Hz, ⁴J_{P-H} = 2.1 Hz, 6H, CH₃), 7.55-7.75 (m, 9H, CH_{Ph meta/para}), 7.82 (m, 8H, CH_{Ph ortho/Py ortho}), 8.81-9.02 (m, 10H, CH_{β-pyrrolic/Py meta}). ³¹P NMR (CDCl₃+DMSO_{d6}, 162 MHz): δ -179. ¹³C NMR (CDCl₃+DMSO_{d6}, 125 MHz): δ 13.1 (CH₃, ²J_{P-C} = 16.2 Hz), 56.9 (CH₂), 112.2 (C), 116.7 (C), 117.0 (C), 128.0 (CH), 128.7 (CH), 129.9 (CH), 130.0 (CH), 132.5 (CH, ³J_{P-C} = 5.0 Hz), 133.4 (CH), 133.5 (CH, ³J_{P-C} = 5.2 Hz), 133.6 (CH, ³J_{P-C} = 5.4 Hz), 134.1 (CH, ³J_{P-C} = 5.1 Hz), 135.1 (CH), 135.2 (C), 138.1 (C), 139.2 (C), 139.3 (C), 139.5 (C), 149.6 (CH). UV-Vis

(CHCl₃) λ, max (nm) (logε, mol⁻¹ L cm⁻¹) 431 (5.16), 559 (3.92), 602 (3.50). HR-ESI MS: *m/z* obsd 367.6361, calcd 367.6376 [(M+H-Br)²⁺]; obsd 734.4825, calcd 734.2679 [(M-Br)⁺]; M = C₄₇H₃₈BrN₅O₂P.

Singlet oxygen and fluorescence experiments.

CHCl₃ was distilled over CaH₂; DMSO was frozen in a fridge (+4 °C), liquid phase was removed and residual solid was melted back; water was distilled with a standard distiller.

The photoluminescence spectra (λ_{ex} = 550 nm) at 25 °C were recorded in quartz cells on a Horiba Scientific Fluorolog spectrofluorimeter. Fluorescence quantum yields (Φ_F) were determined by a comparative method using **Eq. (1)**:

$$\Phi_F = \Phi_F^{St} \frac{F \cdot A^{St} \cdot n^2}{F^{St} \cdot A \cdot n_{St}^2} \quad (1)$$

where Φ_FSt is fluorescence quantum yield of the standard, F and FSt areas under the fluorescence emission peaks of the samples and the standard, respectively; A and ASt are absorptions of the sample and the standard at the excitation wavelengths, respectively; n² and n_{St}² are the refractive indices of solvents used for the sample and the standard, respectively. **1a** in toluene (Φ_F = 0.11)³ was used as a standard.

A special experimental setup was constructed for singlet oxygen quantum yield determination experiments. Two modifications of it was used for organic and aqueous media.

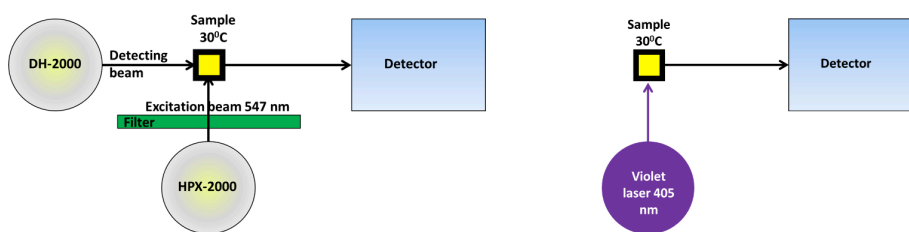


Figure S1 Experimental setups for SO measurements in organic (left) and aqueous (right) media.

In case of organic solvents and DPBF as a singlet oxygen sensitive trap (**Fig. 2, Fig. S30-S31**), a Xenon lamp (HPX-2000, Ocean Optics), equipped with a narrow green filter (transmission maximum at 547 nm) was used for irradiation of the sample. A halogen lamp, equipped with an attenuator, (DH-2000, Ocean Optics) and a detector (in absorption mode) was installed orthogonally. Absorption spectra were registered every 2 sec. **1a** in chloroform (Φ_Δ = 0.50)⁴ was used as a reference. In case of aqueous solutions and SOSG as a singlet oxygen

sensitive trap (**Fig. 2**), a violet semi-conducting laser (405 nm, STAR405F10, Roithner Laser Technik) was used for irradiation of the sample. The detector was switched to emission mode and connected orthogonally. Emission spectra were registered every 5 sec. 5,10,15,20-tetra(4-sulfonatophenyl)-porphyrin in water ($\Phi_{\Delta} = 0.64$)⁵ was used as a reference.

Samples were prepared in open quartz cells in 2.4 ml of the solvent with the concentration $ca \sim 10^{-6}$ M; c (DPBF) = 5×10^{-5} M; c (SOSG) = 1.16×10^{-3} M. Each sample was measured at 30 °C with permanent stirring. Solutions were not degassed or extra bubbled with air (oxygen), thus concentration of O₂ was close to literature values: 0.742 mole fraction at 30 °C and 100 kPa.⁶

Quantum yields of singlet oxygen generation (Φ_{Δ}) were determined by a comparative method using **Eq. (2)**:

$$\Phi_{\Delta} = \Phi_{\Delta}^{St} \frac{R \cdot I^{St}}{R^{St} \cdot I} \quad (2)$$

where Φ_{Δ}^{St} is the singlet oxygen quantum yield of the standard; R and R^{St} are rates of DPBF photobleaching (or SOSG luminescence increasing) in the presence of the sample and the standard, respectively; I and I^{St} are the integral light absorption values of the sample and the standard, respectively.

The solution of investigated porphyrin mixed with DPBF has an overlapped spectrum (**Fig. 2**) – Soret-band and DPBF-band are located in the same area. The exception is complex **2a**: two individual peaks are observed (**Fig. S30**), since Soret-band undergoes significant bathochromic shift after complexation with phosphorus. Free-base TPP **1a** was used as a standard with known quantum yield of singlet oxygen generation. Porphyrins were irradiated into Q-bands area with Xenon lamp equipped with narrow filter (547 nm). This region also avoids direct influence to DPBF and its photodegradation.⁷ Moreover, in chloroform experiments, negative factors of its irradiation and further formation of phosgene and hydrochloric acid were avoided.

In case of aqueous solution, it is not possible to use previous scheme of the setup anymore, since SOSG-EP emits at 530 nm. Thus, samples in water were irradiated with violet laser 405 nm. Fluorescence of SOSG-EP was registered and used for further calculations (**Fig. 2**). Using described methods and procedures, values of singlet oxygen generation quantum yields for eight

different P(V) porphyrins are calculated and given in the table 1. Since complexes **2** hydrolyze in the presence of moisture they were not involved into investigations in distilled water.

Transient absorption spectroscopy experiments.

Transient absorption spectra were measured by the femtosecond pump to supercontinuum probe setup. The output of a Ti: sapphire oscillator (800 nm, 80 MHz, 80 fs, «Tsunami», «Spectra-Physics», USA) was amplified by a regenerative amplifier system («Spitfire», «Spectra-Physics», USA) at the repeating rate of 1 KHz. Frequency control of laser pulses was produced by regular device synchronization and control amplifier SDG II Spitfire 9132, manufactured by Spectra-physics (USA). The device allowed to change the pulse repetition frequency of the amplifier output from 0 to 1000 Hz. The amplified pulses were split into two beams. One of the beams was directed into a noncollinearly phase-matched optical parametric amplifier. The gauss pulses of 20 fs, 30 nJ at 620 nm were used as a pump. The second beam was focused onto a thin quartz cell with water to generate supercontinuum probe pulses. The pump and probe pulses were time-delayed with respect to each other using a computer-controlled delay stage. They were then attenuated, recombined, and focused onto the sample cell. The pump and probe light spots had the diameters of 300 and 120 μm , respectively.

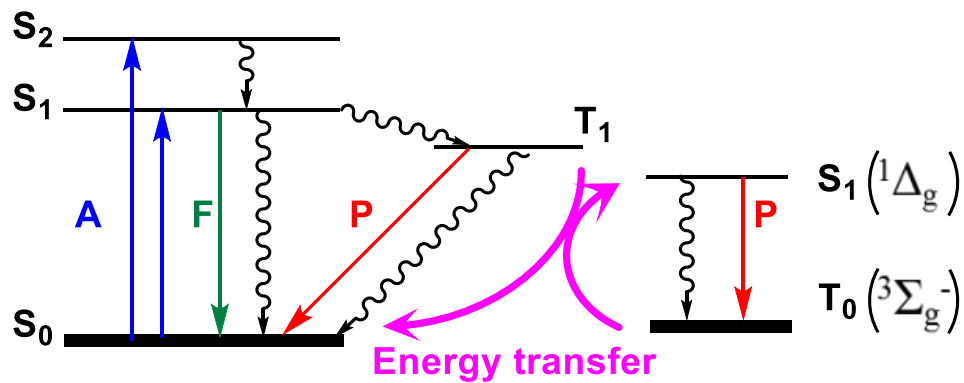
Experiments were carried out at 278 K in acetonitrile. The pump pulse operation frequency was 60 Hz, which is sufficiently low to exclude permanent bleaching of the sample due to photochemical processes in the sample. The relative polarizations of pump and probe beams were adjusted to 54.7° (magic angle) or in parallel and perpendicular polarizations, where indicated. After the sample, the supercontinuum was dispersed by a polychromator («Acton SP-300») and detected by CCD camera («Roper Scientific SPEC-10»). Transient spectra of absorbance changes $\Delta A(t, \lambda)$ were recorded over the range of 380–800 nm. The measured spectra were corrected for group delay dispersion of the supercontinuum using the procedure described previously.⁸

Table S1 Stokes shifts and emission maxima of P(V) porphyrins.

Complex	Chloroform		DMSO		Water	
	λ_F , nm	Stoke shift, nm	λ_F , nm	Stoke shift, nm	λ_F , nm	Stoke shift, nm
2a	622, 677	109	625, 679	111	hydrolysis	
3a	609, 664	106	614, 667	109	614, 667	112
4a	619, 672	107	618, 668	103	619, 671	107
5a	610, 663	106	614, 666	109	621, 673	115
2b	621, 676	110	624, 678	111	hydrolysis	
3b	611, 663	107	612, 667	110	614, 667	113
4b	621, 671	107	617, 666	100	616, 667	104
5b	616, 669	110	618, 671	111	618, 674	117

Table S2 Quantum yields of S_1-S_0 , S_1-CT and S_1-T_1 processes calculated from transient absorption experiments.

Complex	Quantum yield of S_1-S_0 transition	Quantum yield of S_1-CT transition	Quantum yield of S_1-T_1 transition
2a	0.15	-	0.86
2b	0.27	-	0.75
3a	0.39	-	0.61
3b	<0.1	-	0.95
4a	0.50	0.40	0.10
4b	0.44	0.39	0.20
5a	0.29	-	0.70
5b	0.11	-	0.89



Scheme S1 Jablonski diagram of energy transitions in photosensitive porphyrin; A – absorption, F – fluorescence, P - phosphorescence.

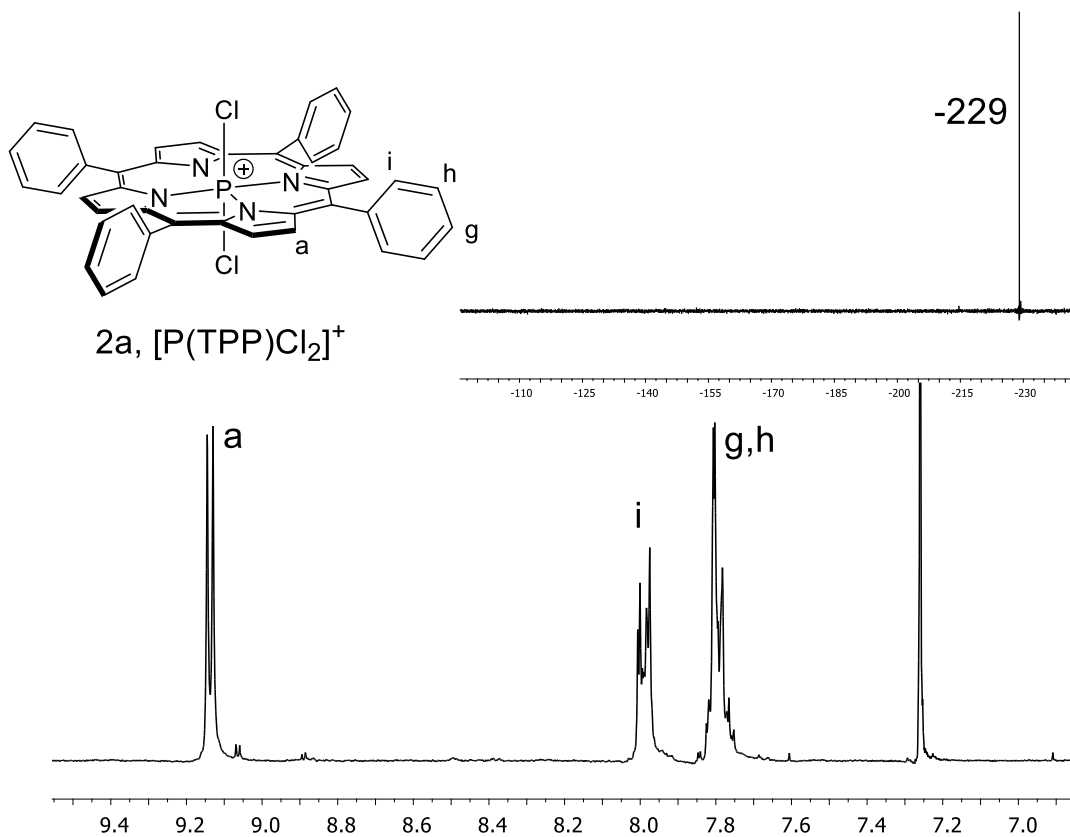


Figure S2 1H -NMR (bottom, $CDCl_3$, 300 MHz, 25 °C) and ^{31}P -NMR (top right, $CDCl_3$, 121 MHz, 25 °C) spectra of **2a**.

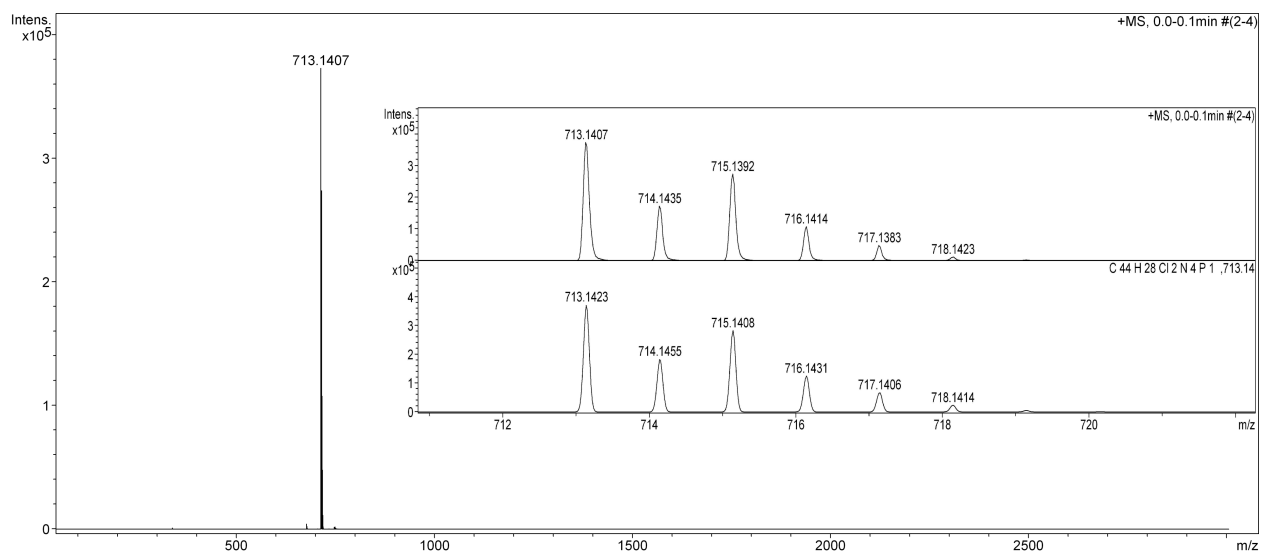


Figure S3 HR-ESI TOF spectrum of **2a**.

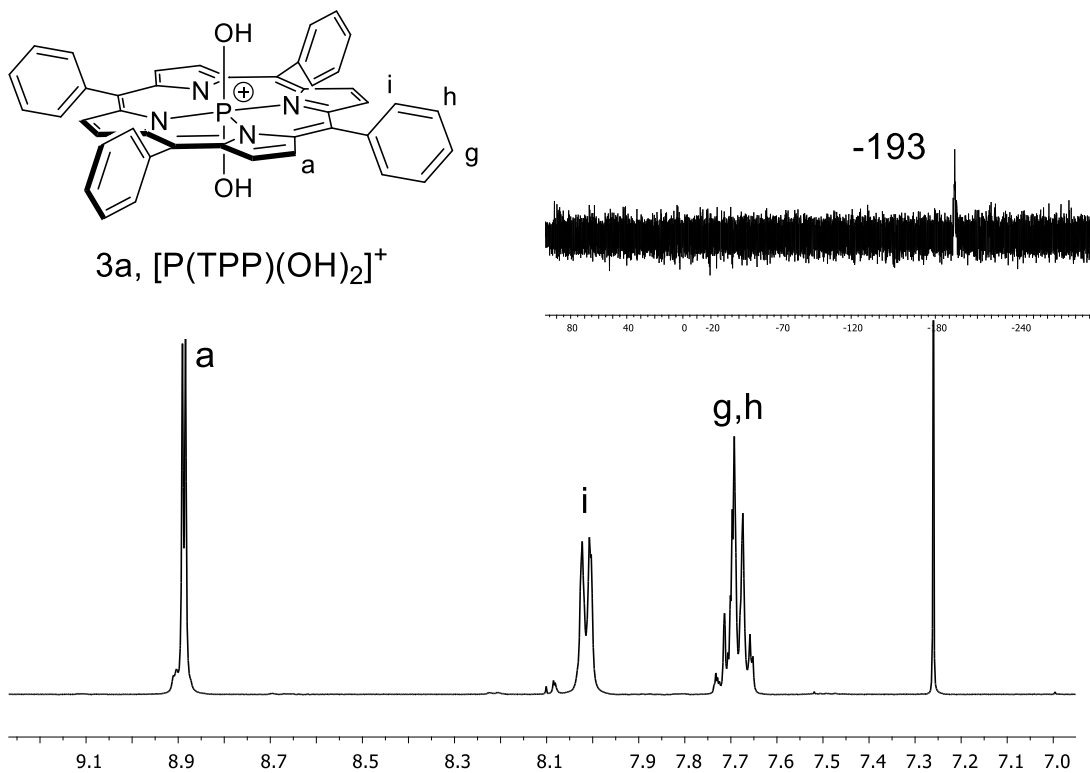


Figure S4 ¹H-NMR (bottom, CDCl₃, 400 MHz, 25 °C) and ³¹P-NMR (top right, CDCl₃, 162 MHz, 25 °C) spectra of **3a**.

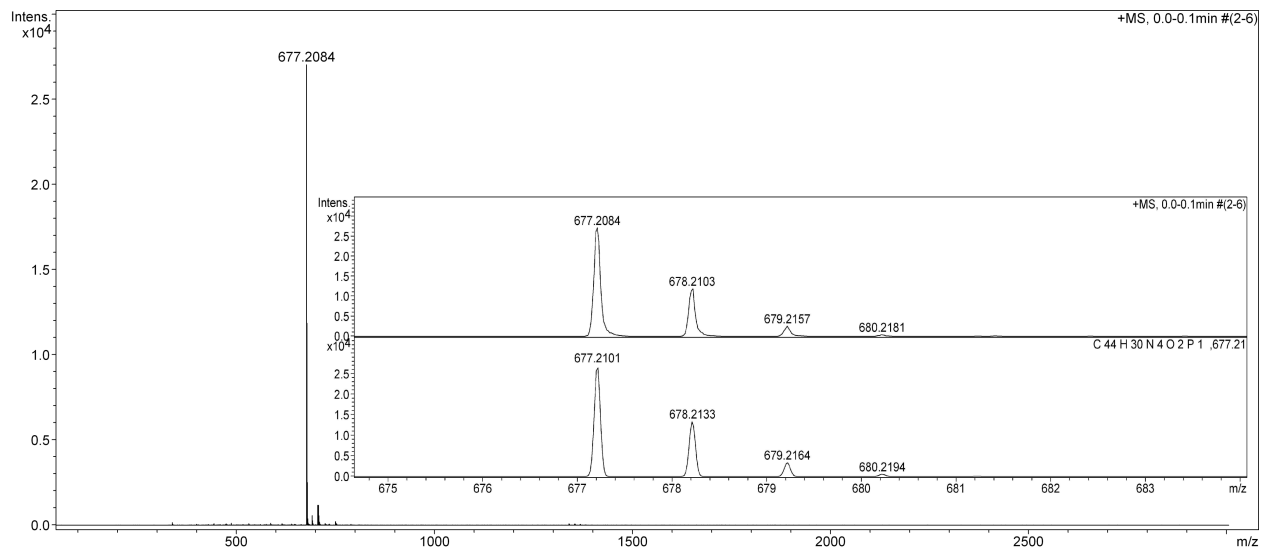


Figure S5 HR-ESI TOF spectrum of **3a**.

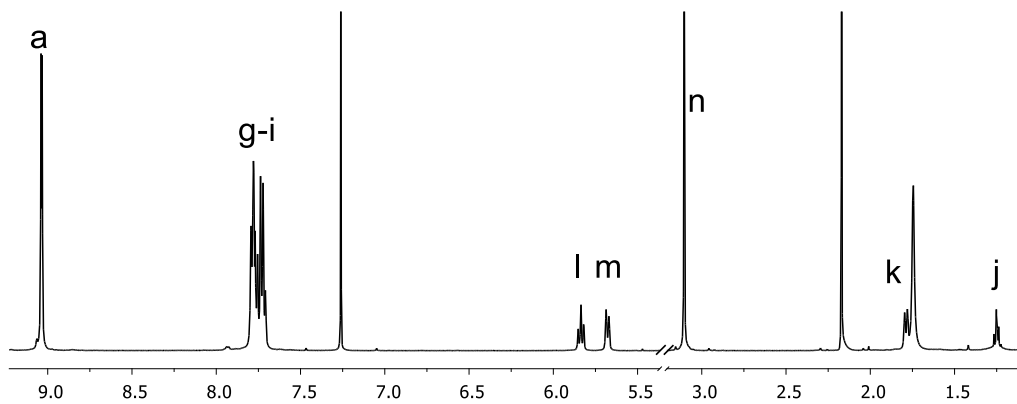
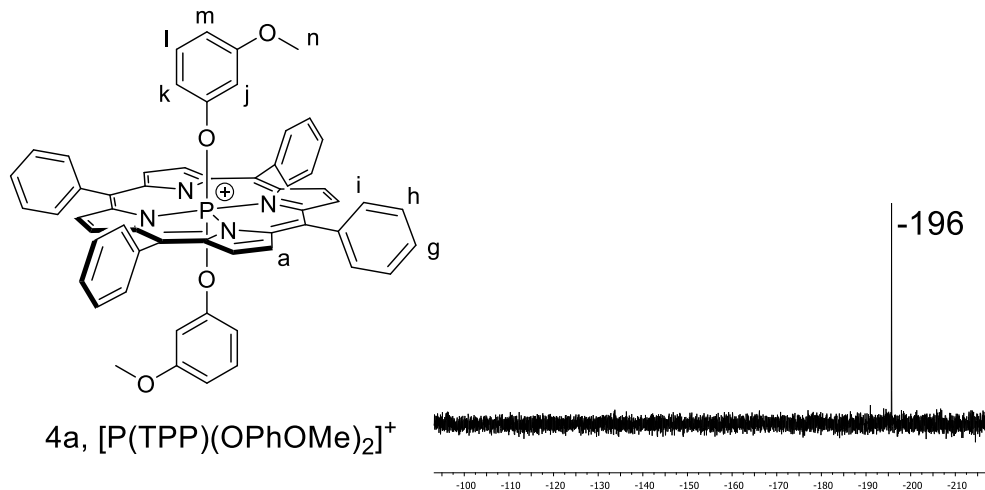


Figure S6 ¹H-NMR (bottom, CDCl₃, 500 MHz, 25 °C) and ³¹P-NMR (top right, CDCl₃, 121 MHz, 25 °C) spectra of **4a**.

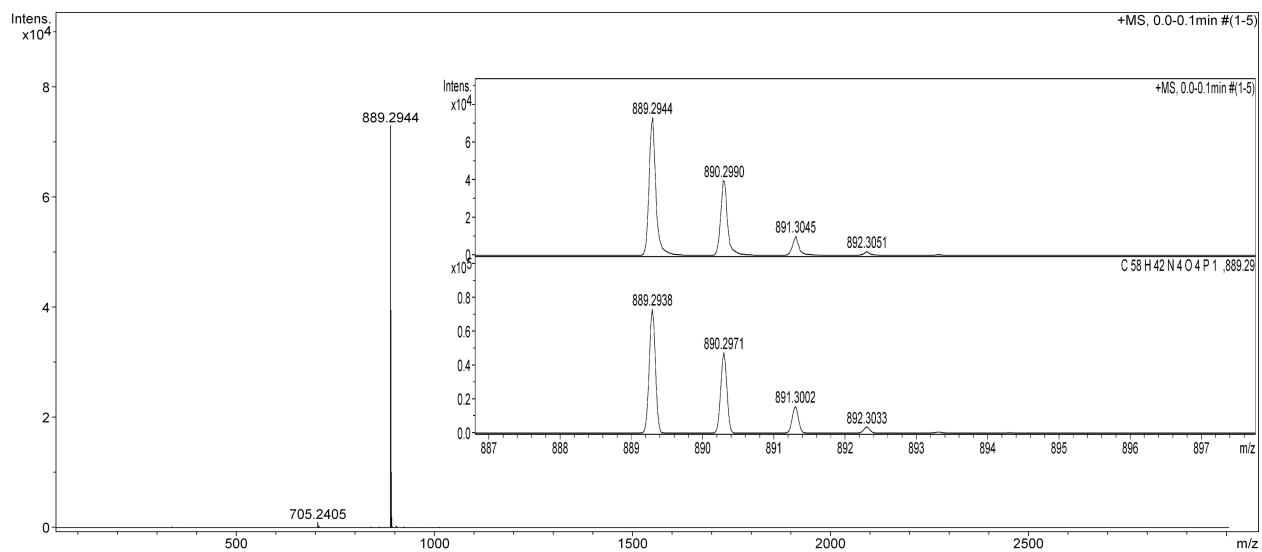


Figure S7 HR-ESI TOF spectrum of **4a**.

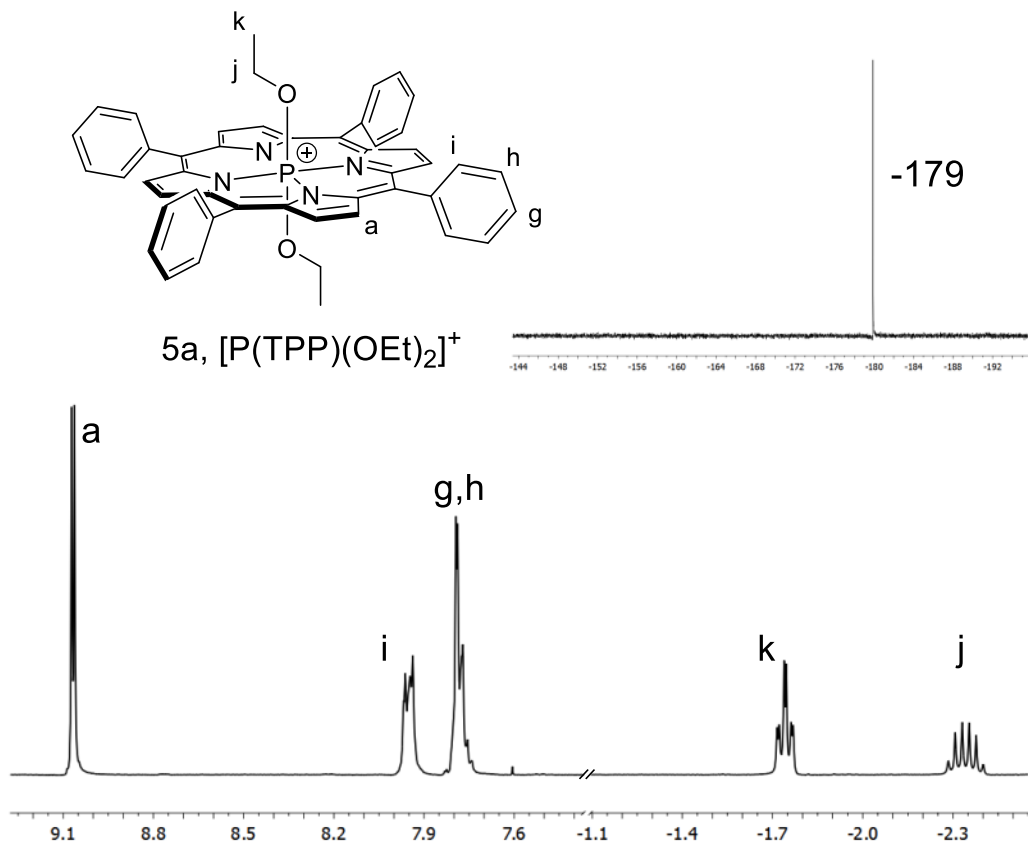


Figure S8 ¹H NMR (bottom, CDCl₃, 300 MHz, 25 °C) and ³¹P NMR (top right, CDCl₃, 162 MHz, 25 °C) spectra of the compound **5a**.

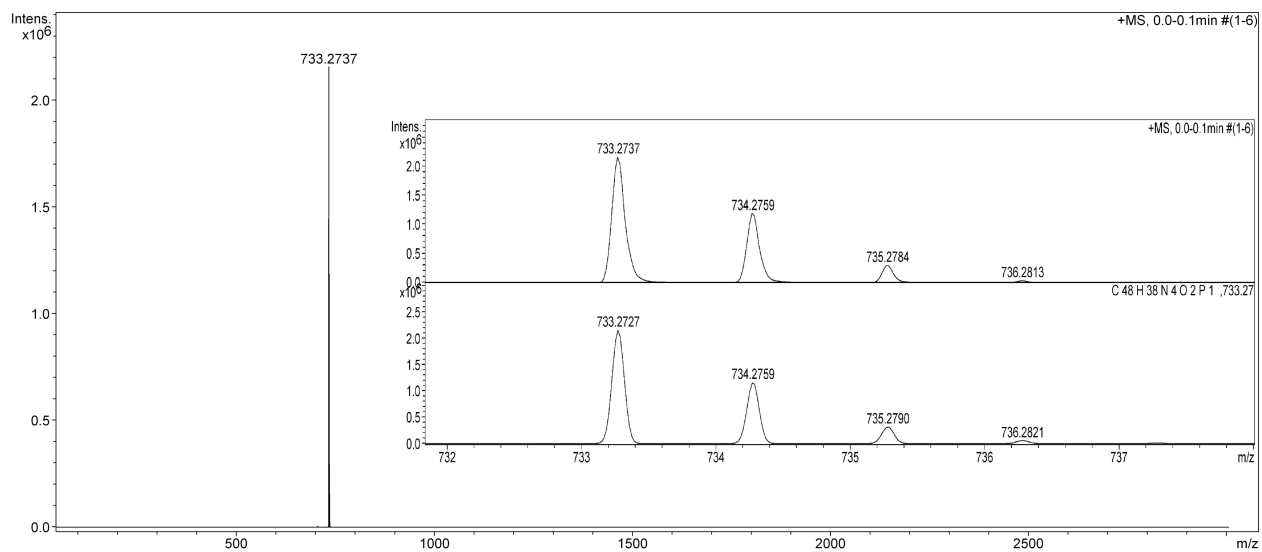


Figure S9 HR-ESI TOF spectrum of the compound **5a**.

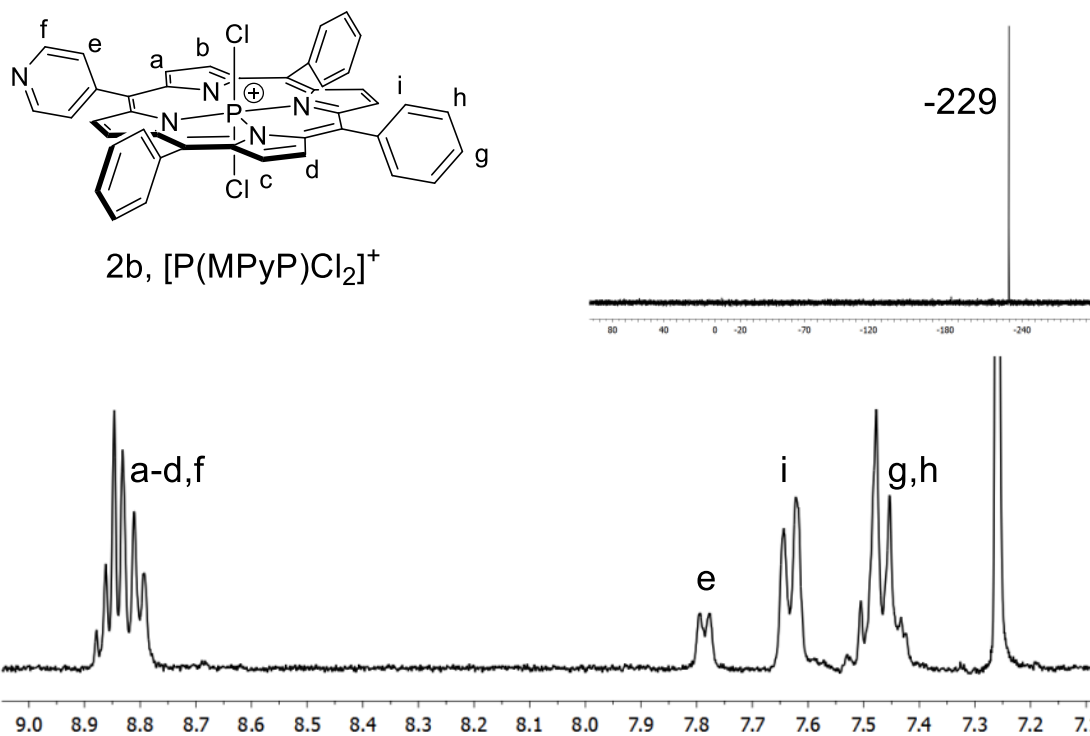


Figure S10 ¹H-NMR (bottom, CDCl₃, 300 MHz, 25 °C) and ³¹P-NMR (top right, CDCl₃, 121 MHz, 25 °C) spectra of **2b**.

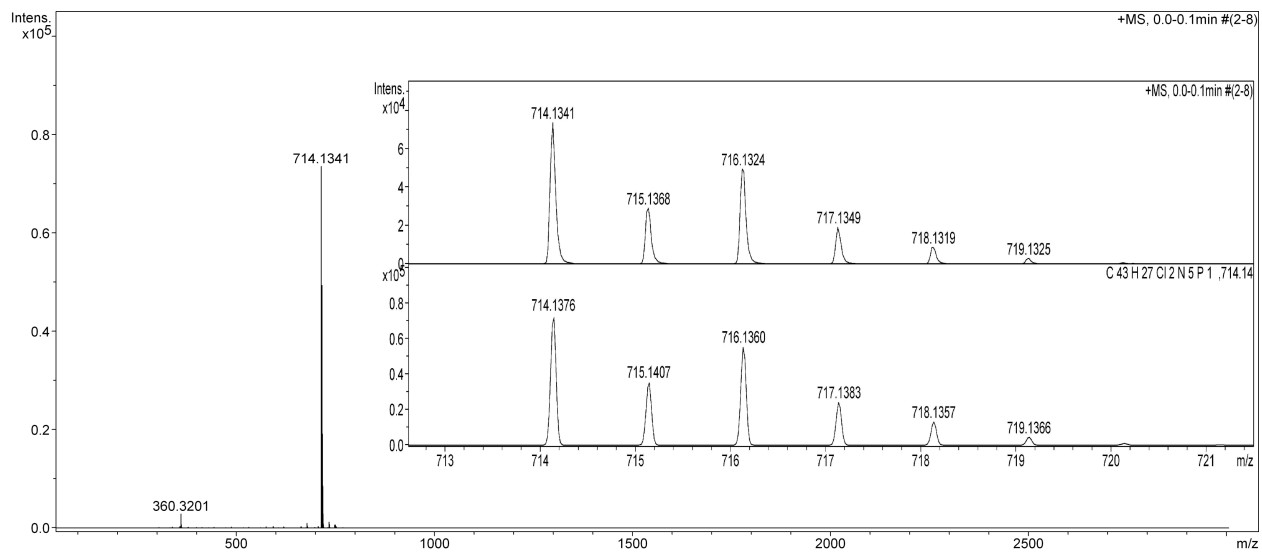


Figure S11 HR-ESI TOF spectrum of **2b**.

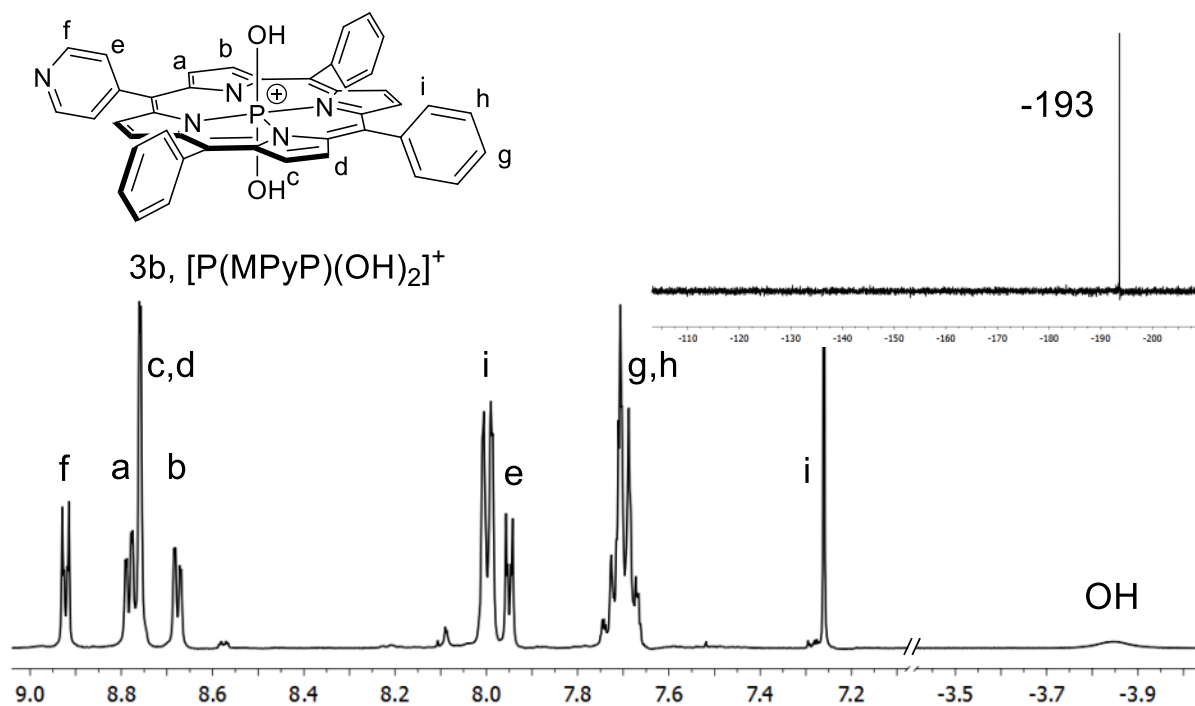


Figure S12 1H -NMR (bottom, $CDCl_3$, 400 MHz, 25 °C) and ^{31}P -NMR (top right, $CDCl_3$, 162 MHz, 25 °C) spectra of **3b**.

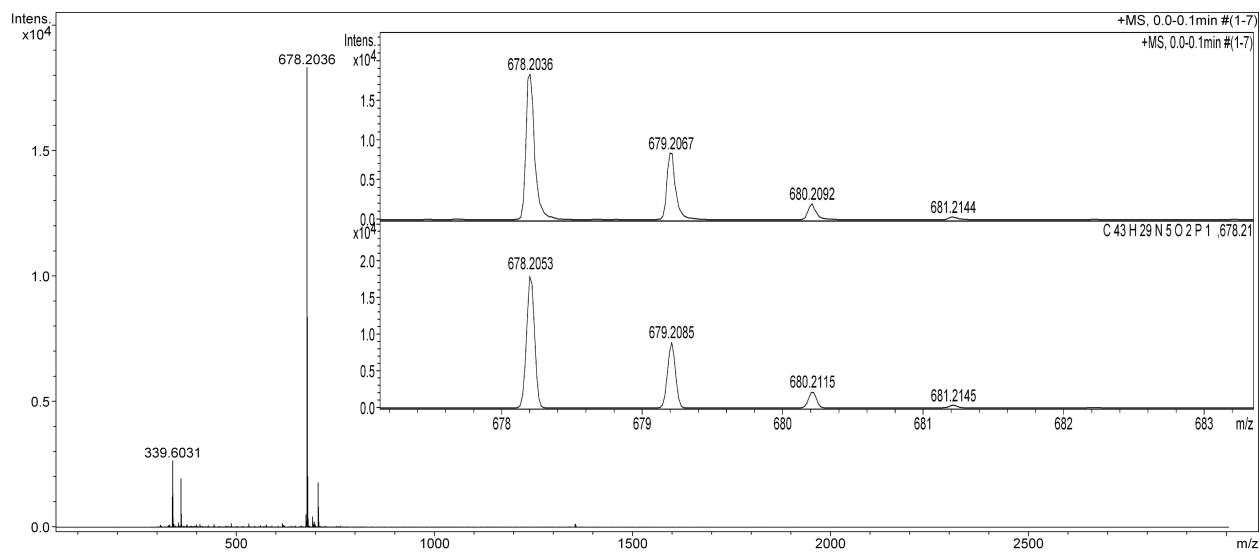


Figure S13 HR-ESI TOF spectrum of **3b**.

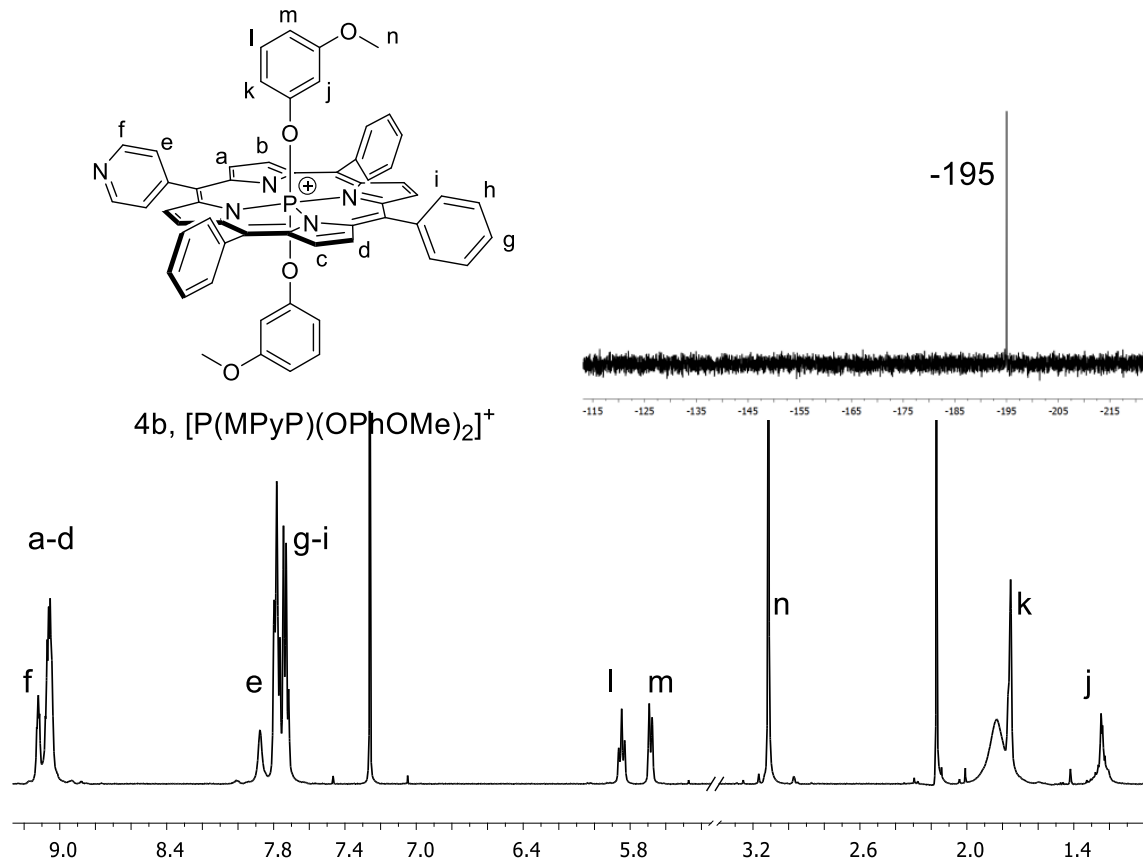


Figure S14 ¹H-NMR (bottom, CDCl₃, 400 MHz, 25 °C) and ³¹P-NMR (top right, CDCl₃, 162 MHz, 25 °C) spectra of **4b**.

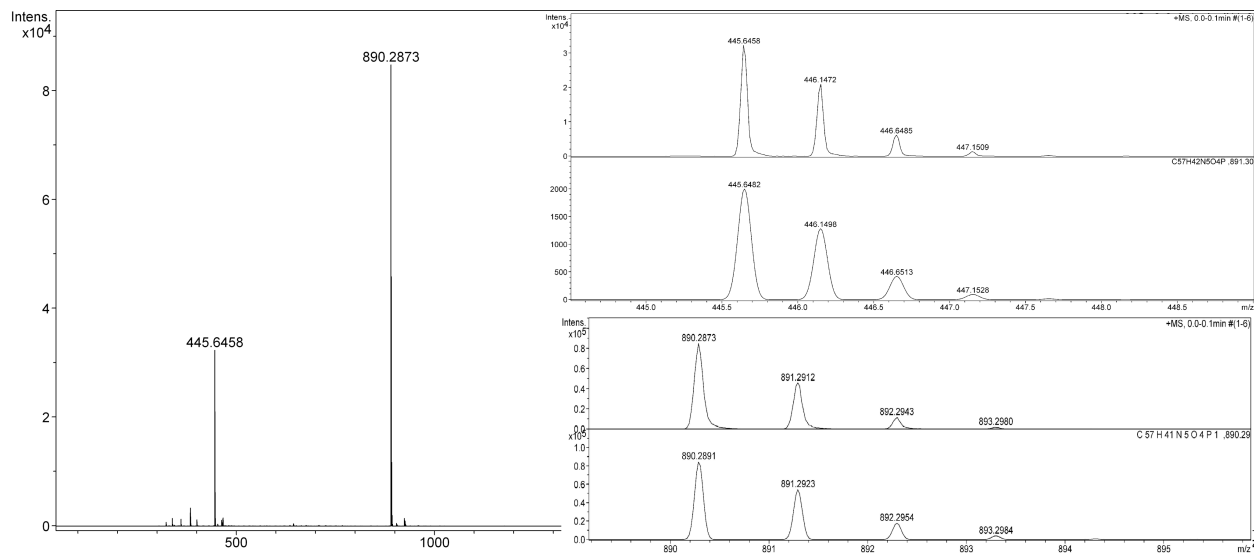


Figure S15 HR-ESI TOF spectrum of **4b**.

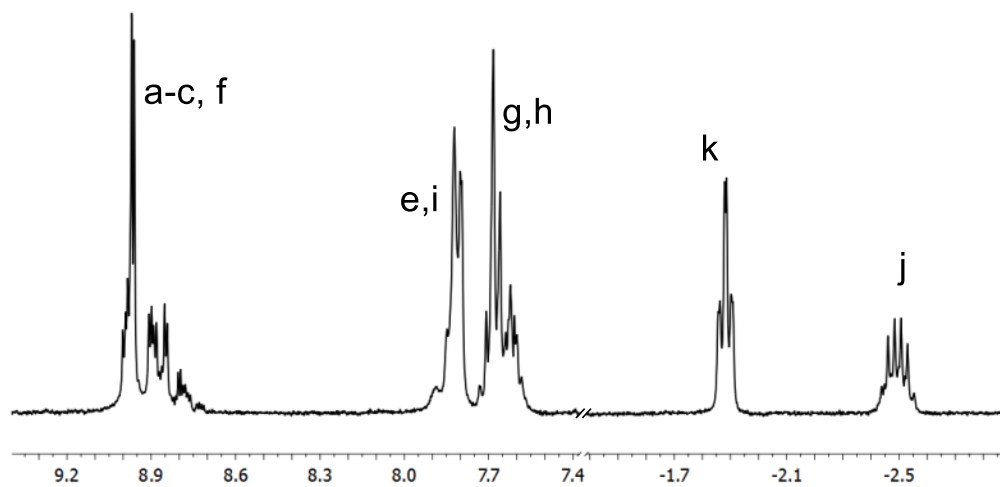
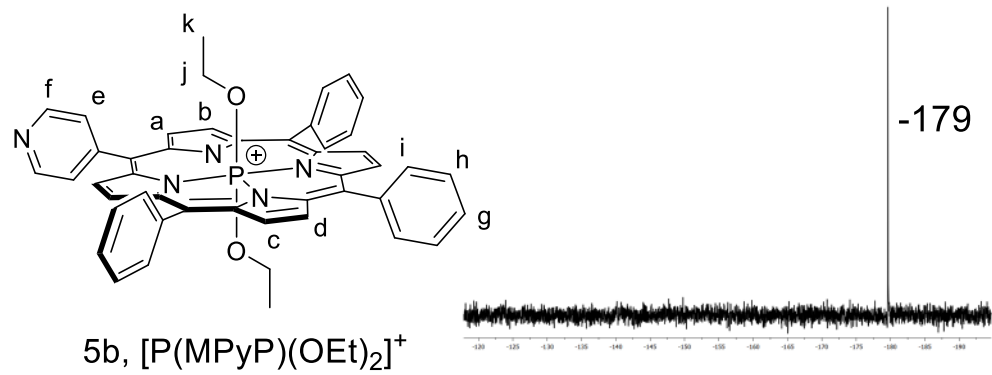


Figure S16 1H NMR (bottom, $CDCl_3+DMSO_{d6}$, 300 MHz, 25 °C) and ^{31}P NMR (top right, $CDCl_3+DMSO_{d6}$, 162 MHz, 25 °C) spectra of the compound **5b**.

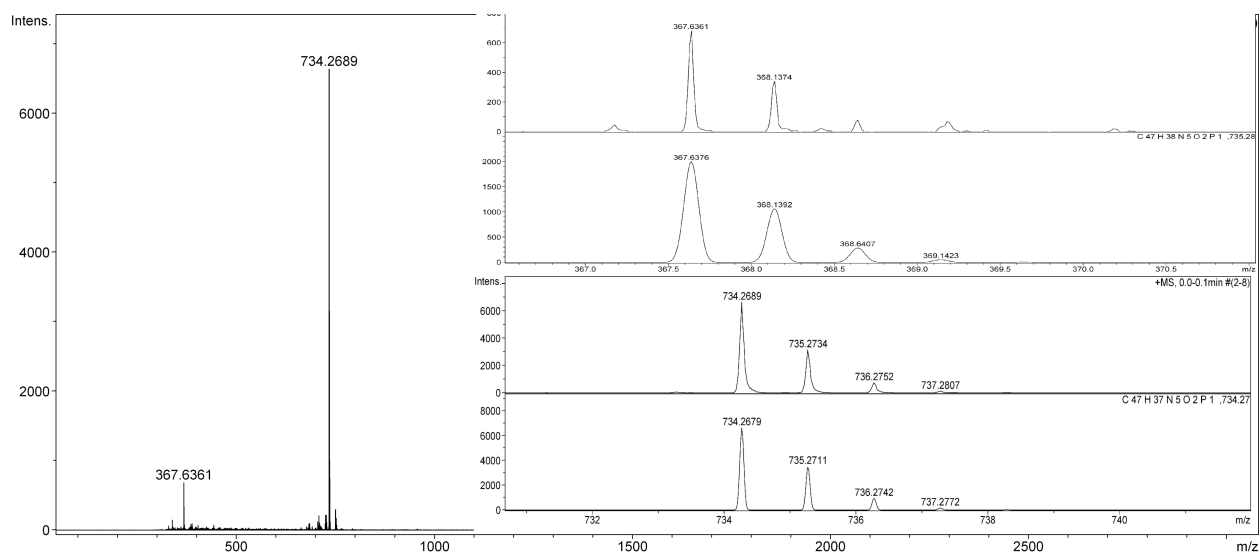


Figure S17 HR-ESI TOF spectrum of the compound **5b**.

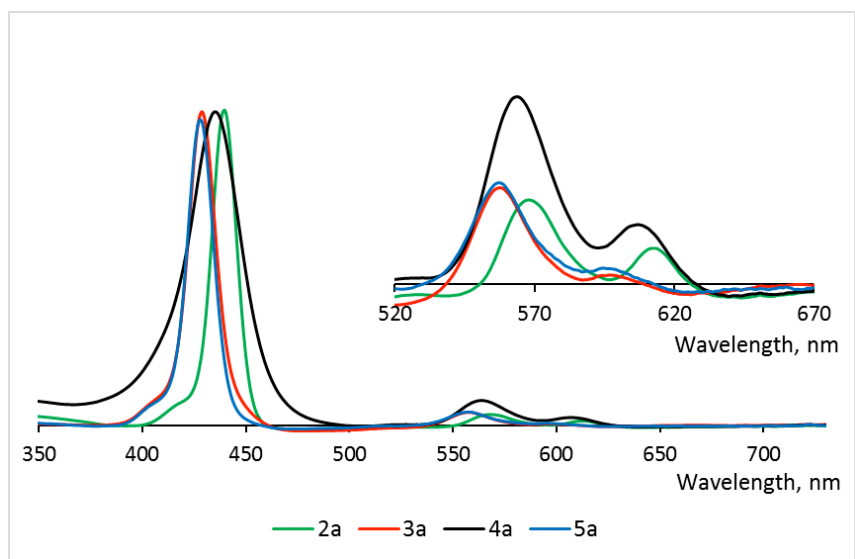


Figure S18 Normalized UV-Vis spectra of compounds **2a-5a** in CHCl_3 .

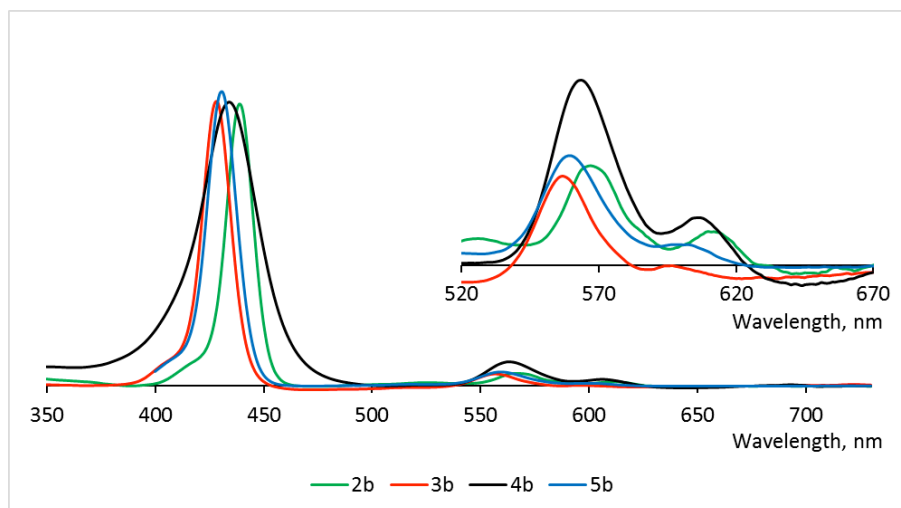


Figure S19 Normalized UV-Vis spectra of compounds **2b-5b** in CHCl_3 .

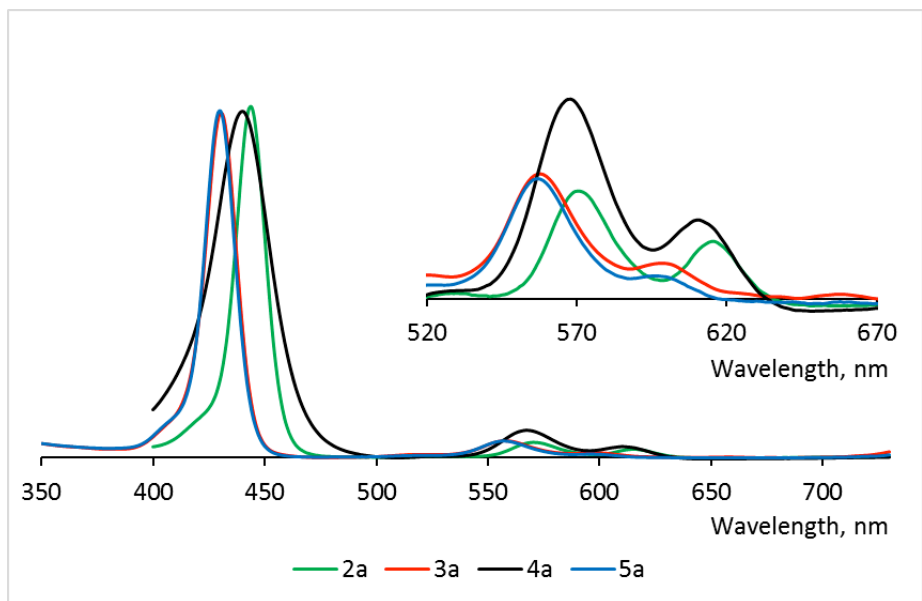


Figure S20 Normalized UV-Vis spectra of compounds **2a-5a** in DMSO.

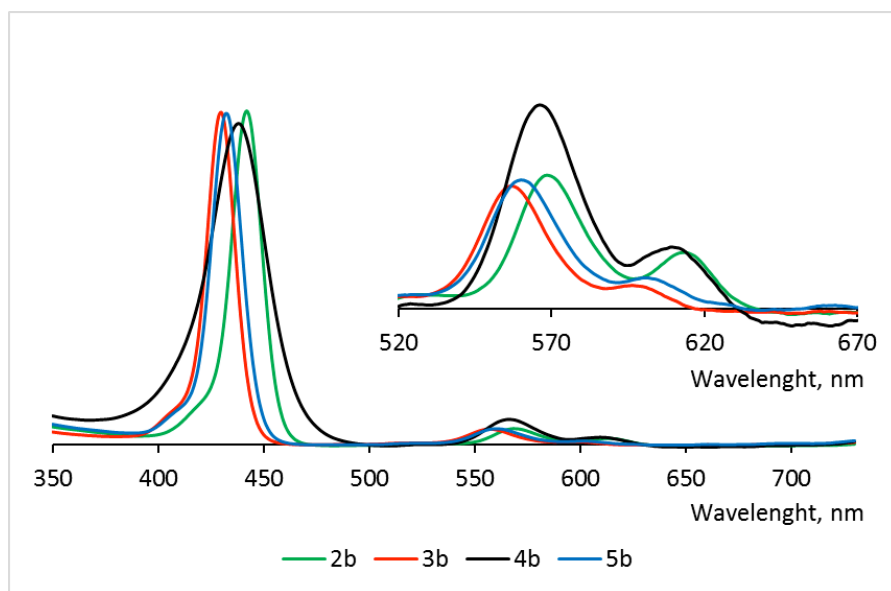


Figure S21 Normalized UV-Vis spectra of compounds **2b-5b** in DMSO.

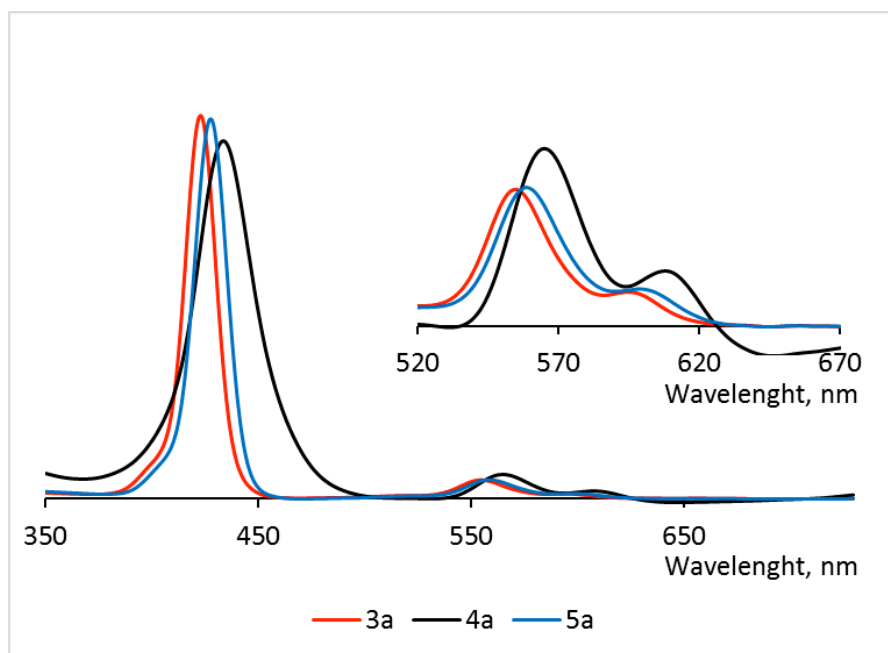


Figure S22 Normalized UV-Vis spectra of compounds **3a-5a** in water.

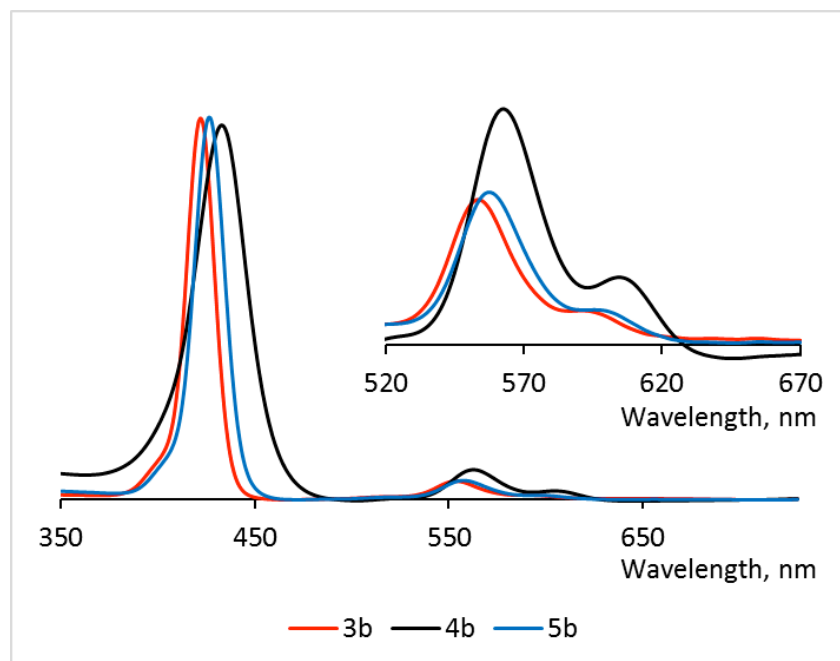


Figure S23 Normalized UV-Vis spectra of compounds **3b-5b** in water.

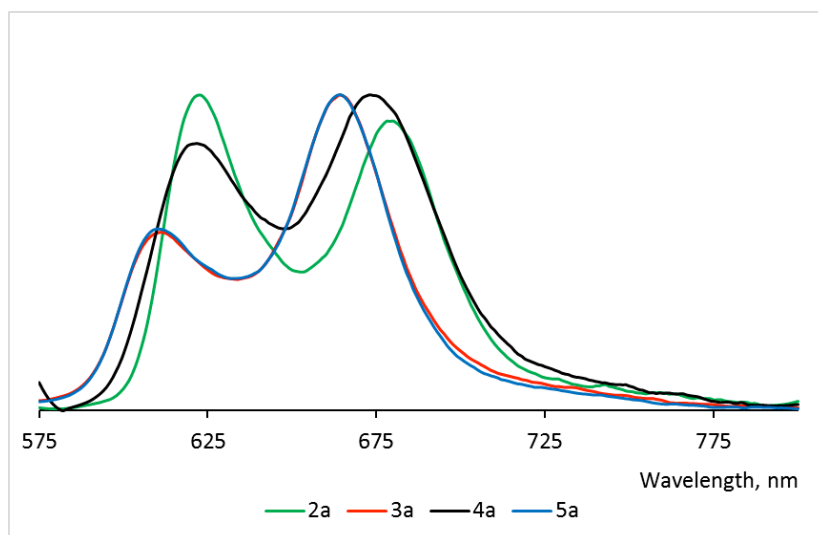


Figure S24 Normalized fluorescence spectra ($\lambda_{\text{ex}} = 550 \text{ nm}$) of compounds **2a-5a** in CHCl₃.

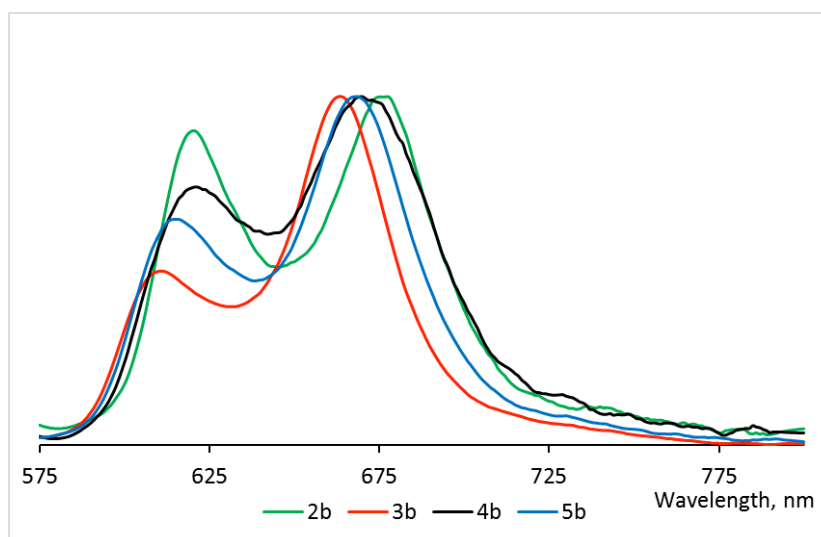


Figure S25 Normalized fluorescence spectra ($\lambda_{\text{ex}} = 550 \text{ nm}$) of compounds **2b-5b** in CHCl₃.

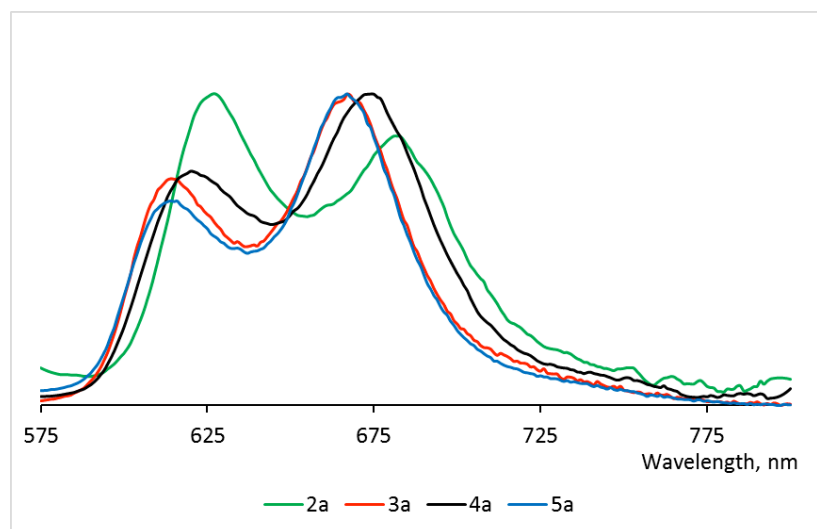


Figure S26 Normalized fluorescence spectra ($\lambda_{\text{ex}} = 550 \text{ nm}$) of compounds **2a-5a** in DMSO.

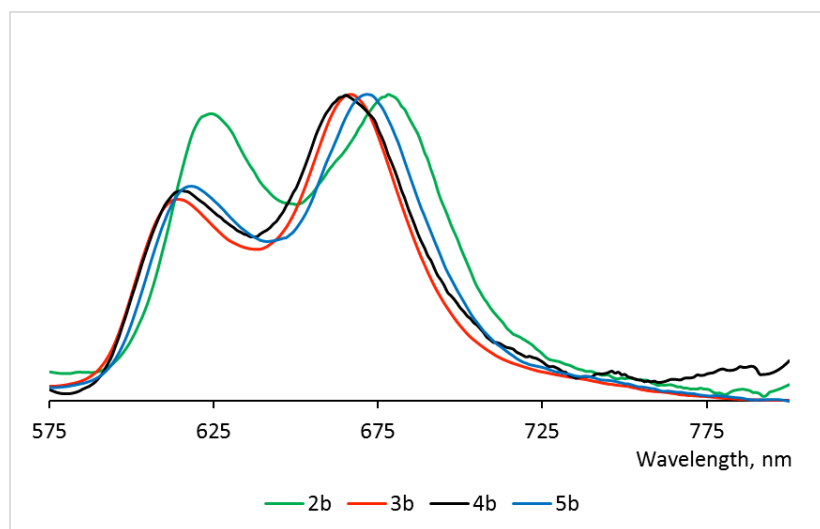


Figure S27 Normalized fluorescence spectra ($\lambda_{\text{ex}} = 550 \text{ nm}$) of compounds **2b-5b** in DMSO.

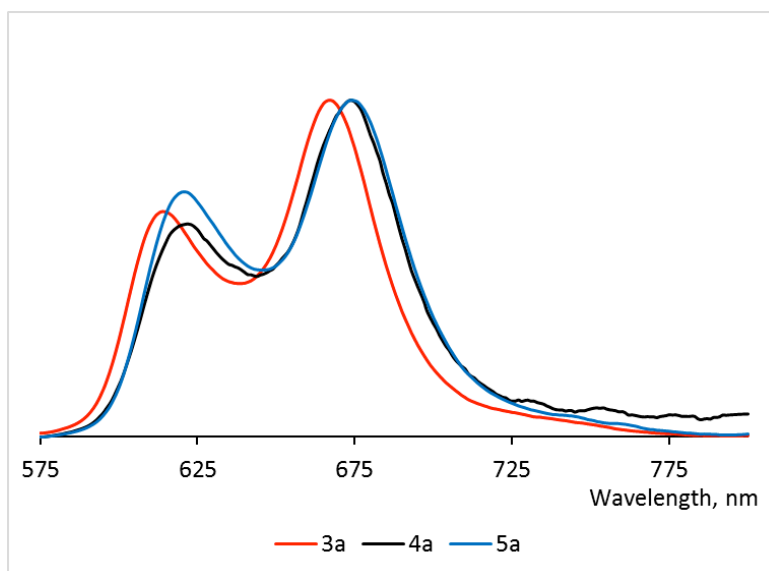


Figure S28 Normalized fluorescence spectra ($\lambda_{\text{ex}} = 550 \text{ nm}$) of compounds **3a-5a** in water.

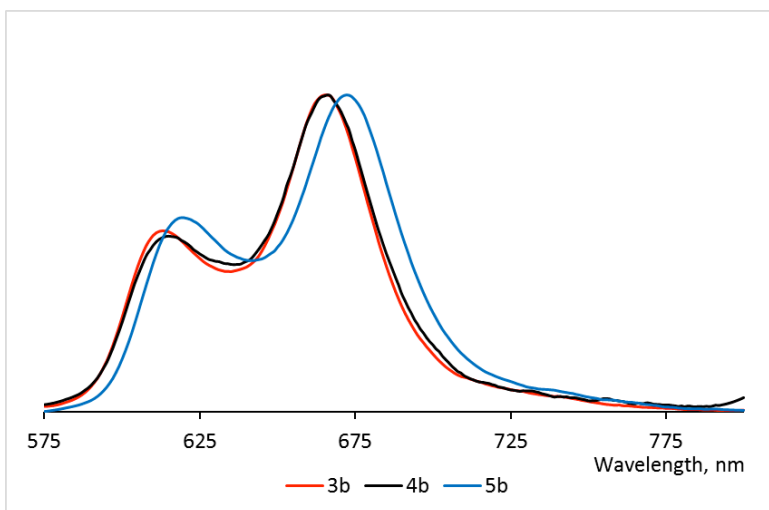


Figure S29 Normalized fluorescence spectra ($\lambda_{\text{ex}} = 550 \text{ nm}$) of compounds **3b-5b** in water.

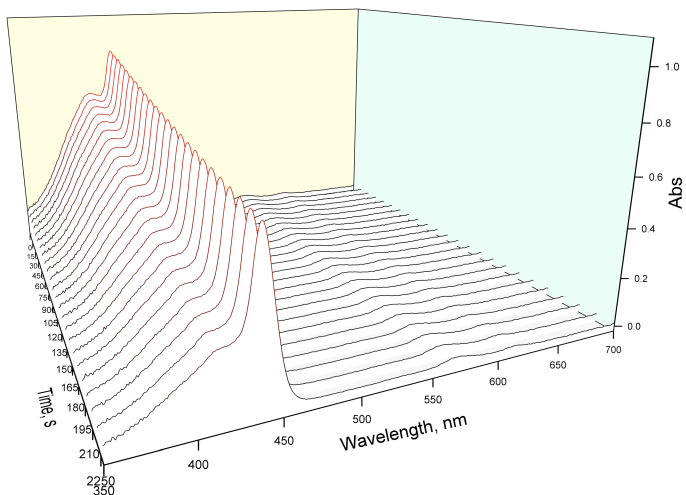


Figure S30 Degradation of DPBF in the chloroform solution of **2a**.

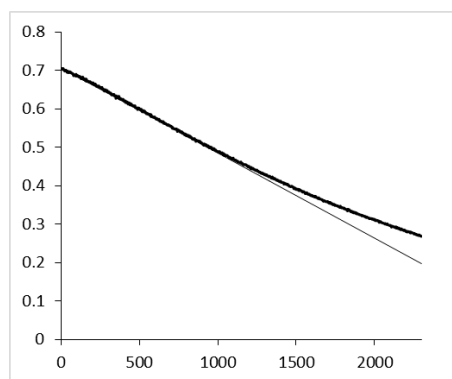


Figure S31 Degradation of DPBF in the chloroform solution of **2a** – plot of DPBF peak (415 nm) vs time.

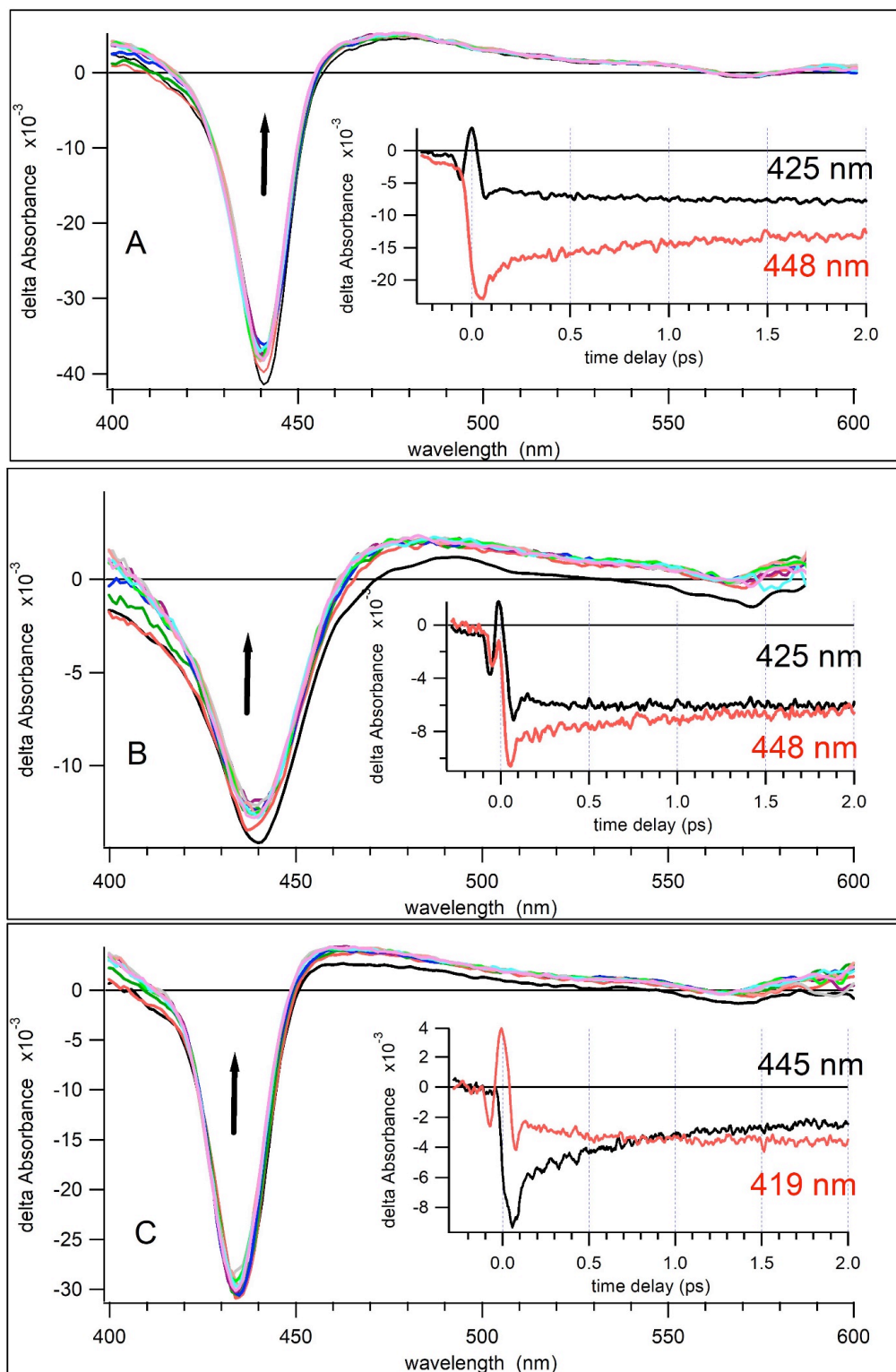


Figure S32 Transient spectra at early time delays. Time delays are shown between 70 fs and 205 fs with the step of 15 fs. Arrows show the rise of time delay. Inserts demonstrates transient traces. (A) - complex **2a**. (B) complex **4a**. (C) complex **5a**.

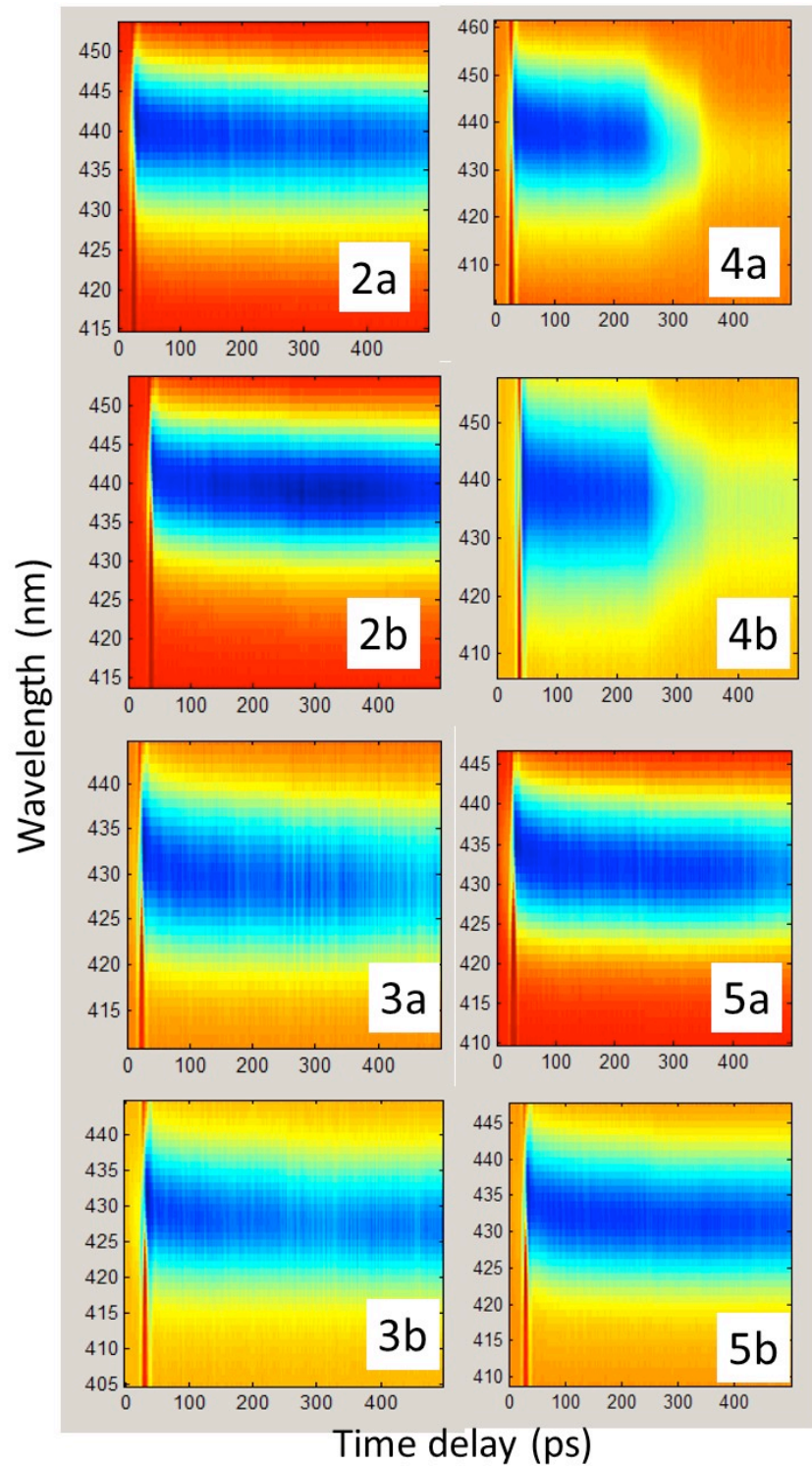


Figure S33 2D maps of transient spectra changes vs time delay.

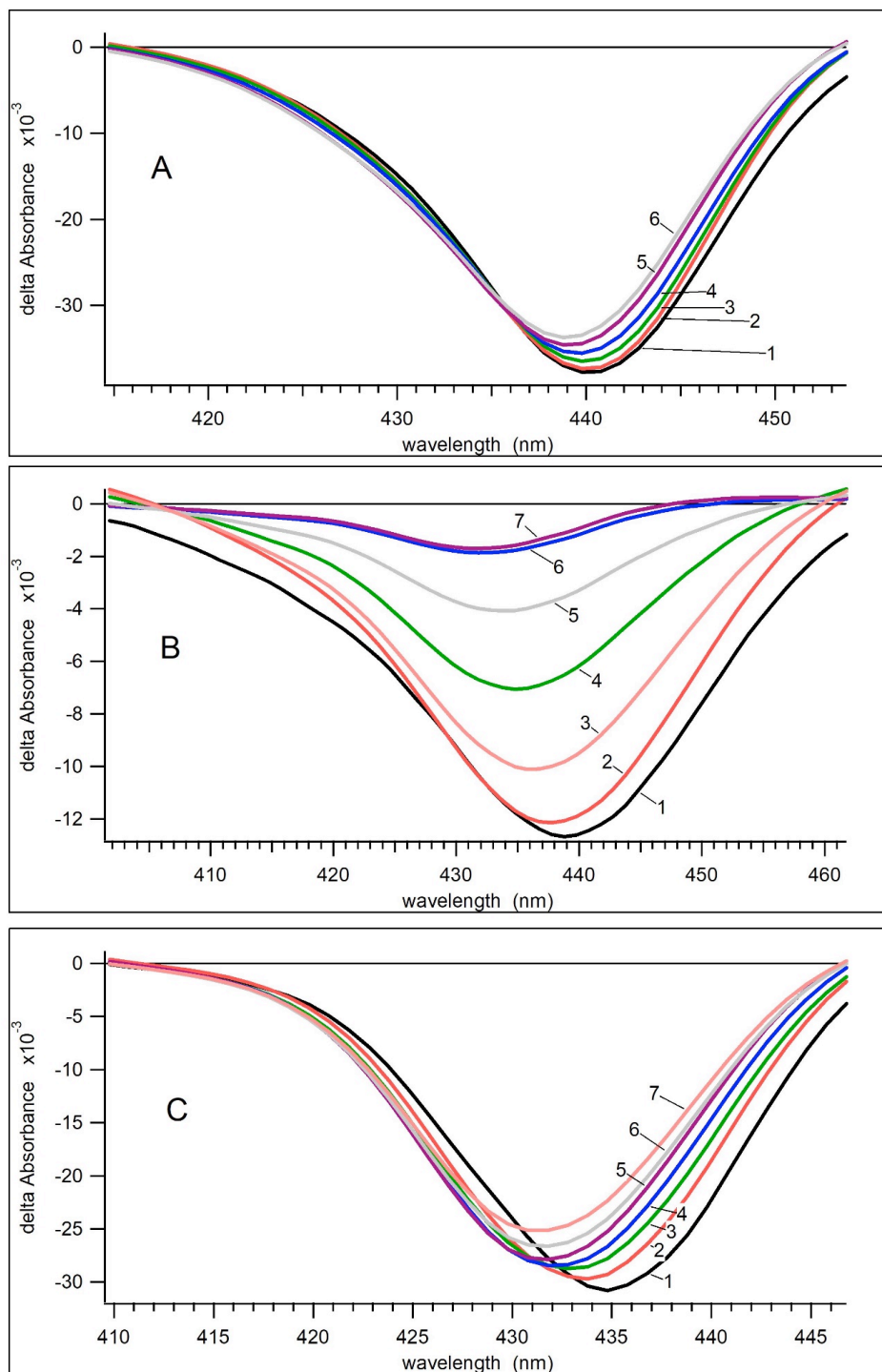


Figure S34 Transient spectra in the region of the Soret band vs time delay. A. **2a**. Time delays: 1) 100 fs; 2) 300 fs; 4) 500 fs; 5) 700 fs; 6) 15 ps; 7) 200 ps. B. **4a**. Time delays: 1) 100 fs; 2) 900 fs; 3) 5 ps; 4) 15 ps; 5) 45 ps; 6) 200 ps; 7) 400 ps. C. **5a**. Time delays: 1) 100 fs; 2) 300 fs; 3) 500 fs; 4) 900 fs; 5) 15 ps; 6) 200 ps; 7) 400 ps.

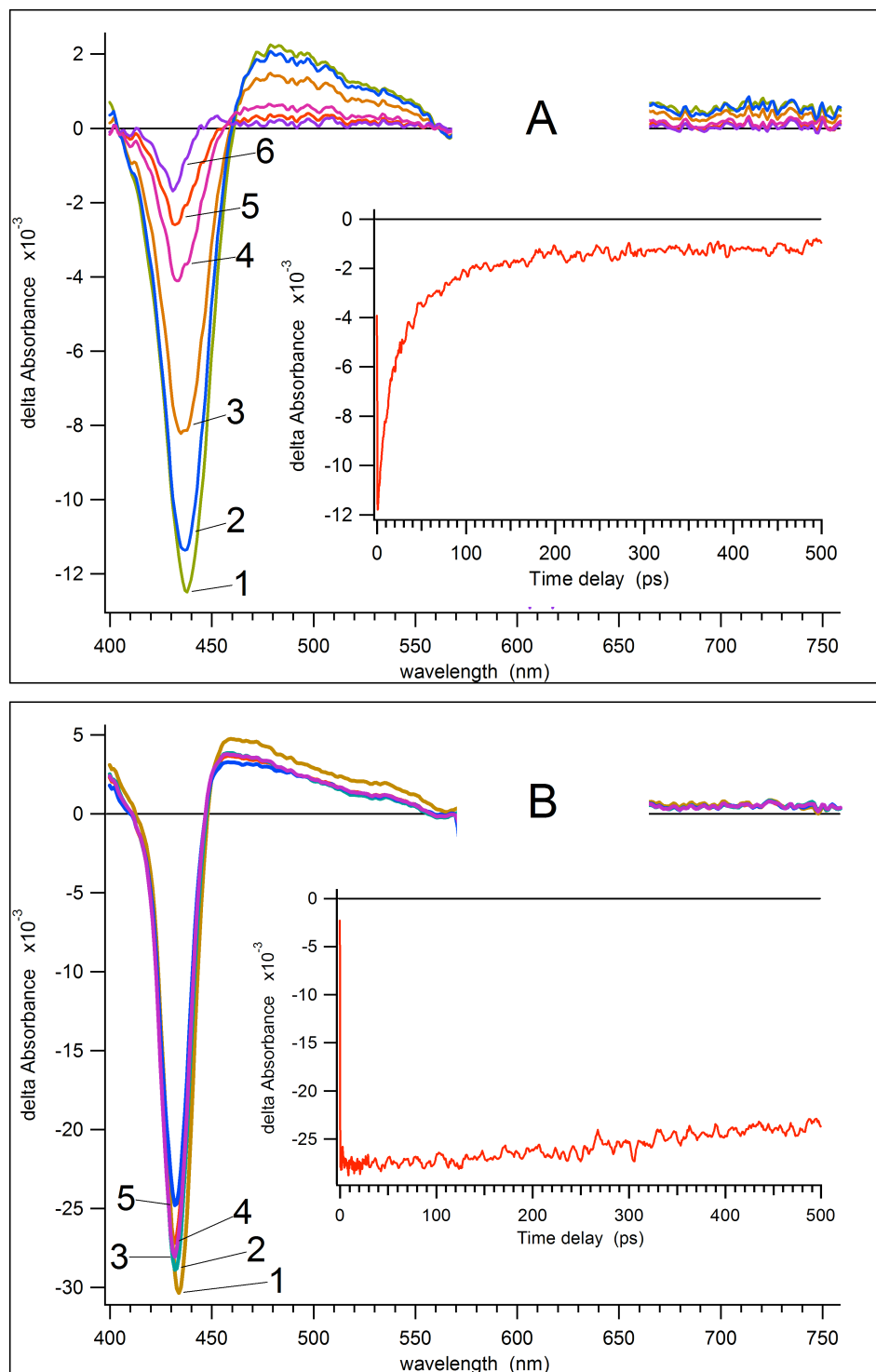


Figure S35 Transient absorption spectra of complexes **4a** (A) and **5a** (B) in acetonitrile ($\lambda_{\text{ex}} = 620$ nm). Time delay (A): 1) 120 fs; 2) 2 ps; 3) 10 ps; 4) 45 ps; 5) 100 ps; 6) 450 ps; time delay (B): 1) 120 fs; 2) 2 ps; 3) 45 ps; 4) 100 ps; 5) 450 ps. Transient kinetics decay are presented in inserts.

Intramolecular energy transitions without CT state for compounds 2, 3 and 5.

Kinetics of the state population.

$$\frac{dS_1}{dt} = -(k_1 + k_2)[S_1]$$

$$\frac{dT_1}{dt} = k_2[S_1]$$

$$\frac{dS_0}{dt} = k_1[S_1]$$

We neglect the transition of $T_1 \rightarrow S_0$ suggesting that it is slow.

$$[S_1](t=0) = C[1]$$

$$[S_1](t) = C[1]e^{-(k_1+k_2)t}$$

$$[T_1] = \frac{k_2}{k_2 + k_1} C[1](1 - e^{-(k_1+k_2)t})$$

Bleaching is directly proportional of the sum S_1+T_1

$$BL = \frac{k_1}{k_2 + k_1} e^{-(k_1+k_2)t} + \frac{k_2}{k_1 + k_2}$$

Fitting

$$Y_0 + A_1 e^{(-t/\tau_1)} :$$

$$\frac{1}{\tau_1} = k_1 + k_2$$

$$A_1 = \frac{k_1}{k_1 + k_2}$$

$$Y_0 = \frac{k_2}{k_1 + k_2}$$

Intramolecular energy transitions with CT state for compounds 4.

Kinetics of the state population.

$$\frac{dS_1}{dt} = -(k_1 + k_2 + k_3)[S_1]$$

$$\frac{dCT}{dt} = k_2[S_1] - k_4[CT]$$

$$\frac{dT_1}{dt} = k_3[S_1]$$

$$\frac{dS_0}{dt} = k_1[S_1] + k_4[CT]$$

We neglect the transition of T1 → S0 suggesting that it is slow.

$$[S_1](t=0) = C[1]$$

$$[S_1] = C[1]e^{-(k_1+k_2+k_3)t}$$

$$[CT] = \frac{e^{-k_4t}(-1 + e^{-(k_1+k_2+k_3)t+k_4t})k_1C[1]}{k_1 + k_2 + k_3 - k_4}$$

$$[T_1] = \frac{(-1 + e^{-(k_1+k_2+k_3)t})k_3C[1]}{k_1 + k_2 + k_3}$$

Bleaching is directly proportional of the sum S₁+CT+T₁

$$BL = \left\{ e^{-(k_1+k_2+k_3)t} - \frac{e^{-k_4t}(-1 + e^{-(k_1+k_2+k_3)t+k_4t})k_1}{k_1 + k_2 + k_3 - k_4} - \frac{(-1 + e^{-(k_1+k_2+k_3)t})k_3}{k_1 + k_2 + k_3} \right\} C[1]$$

$$\left\{ e^{-(k_1+k_2+k_3)t} \left(1 - \frac{k_1}{k_1 + k_2 + k_3 - k_4} - \frac{k_3}{k_1 + k_2 + k_3} \right) + \frac{k_1 e^{-k_4t}}{k_1 + k_2 + k_3 - k_4} + \frac{k_3}{k_1 + k_2 + k_3} \right\} C[1]$$

Fitting

$$Y_0 + A_1 e^{(-t/\tau_1)} + A_2 e^{(-t/\tau_2)}$$

$$Y_0 = \frac{k_3}{k_1 + k_2 + k_3}$$

$$A_1 = 1 - \frac{k_1}{k_1 + k_2 + k_3 - k_4} - \frac{k_3}{k_1 + k_2 + k_3}$$

$$\frac{1}{\tau_1} = k_1 + k_2 + k_3$$

$$A_2 = \frac{k_1}{k_1 + k_2 + k_3 - k_4}$$

$$\frac{1}{\tau_2} = k_4$$

Calculated transient absorption spectra data for complexes 2-5.

Compound 2a.

$$Y_0 = 0.86433 \pm 0.0688$$

$$A = 0.15253 \pm 0.0664$$

$$\tau^{-1} = 0.0011486 \pm 0.000696 \text{ ps}^{-1}$$

Compound 2b.

$$Y_0 = 0.7493 \pm 0.074$$

$$A = 0.27382 \pm 0.0731$$

$$\tau^{-1} = 0.00084358 \pm 0.000276 \text{ ps}^{-1}$$

Compound 3a.

$$Y_0 = 0.61358 \pm 0.0582$$

$$A = 0.39085 \pm 0.0569$$

$$\tau^{-1} = 0.0014321 \pm 0.000289 \text{ ps}^{-1}$$

Compound 3b.

$$Y_0 = 0.94673 \pm 0.176$$

$$A = 2.498\text{e-}16 \pm 0.174$$

Compound 4a.

$$Y_0 = 0.10385 \pm 0.000781$$

$$A_1 = 0.50074 \pm 0.00887$$

$$\tau_1^{-1} = 0.093341 \pm 0.00191 \text{ ps}^{-1}$$

$$A_2 = 0.40357 \pm 0.00896$$

$$\tau_2^{-1} = 0.017502 \pm 0.000402 \text{ ps}^{-1}$$

Compound 4b.

$$Y_0 = 0.20001 \pm 0.00182$$

$$A_1 = 0.43637 \pm 0.028$$

$$\tau_1^{-1} = 0.17928 \pm 0.0116 \text{ ps}^{-1}$$

$$A_2 = 0.39398 \pm 0.0285$$

$$\tau_2^{-1} = 0.034515 \pm 0.00269 \text{ ps}^{-1}$$

Compound 5a.

$$Y_0 = 0.7 \pm 0.0861$$

$$A = 0.28576 \pm 0.0849$$

$$\tau^{-1} = 0.0011498 \pm 0.000443 \text{ ps}^{-1}$$

Compound 5b.

$$Y_0 = 0.88996 \pm 0.0296$$

$$A = 0.11261 \pm 0.0277$$

$$\tau^{-1} = 0.0015286 \pm 0.000594 \text{ ps}^{-1}$$

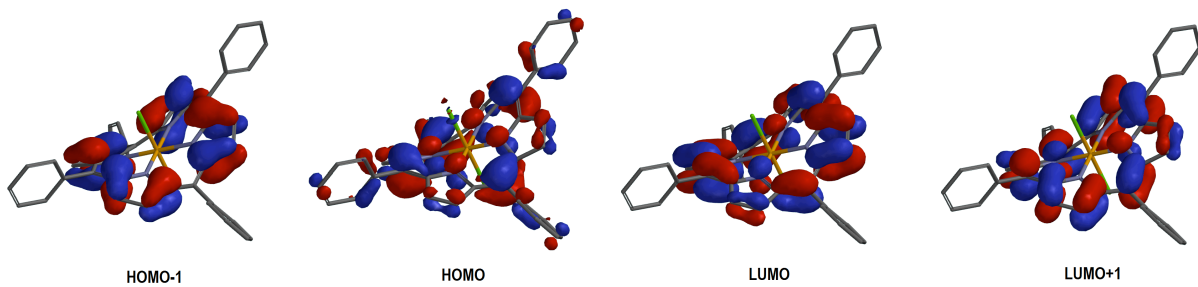


Figure S36 Calculated molecular orbitals of **2a**.

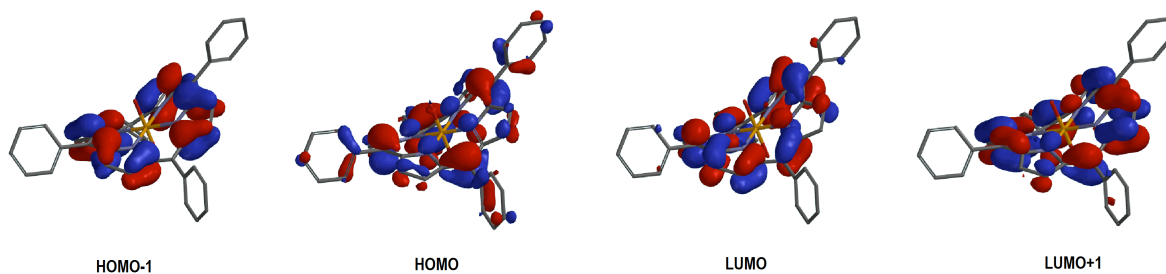


Figure S37 Calculated molecular orbitals of **3a**.

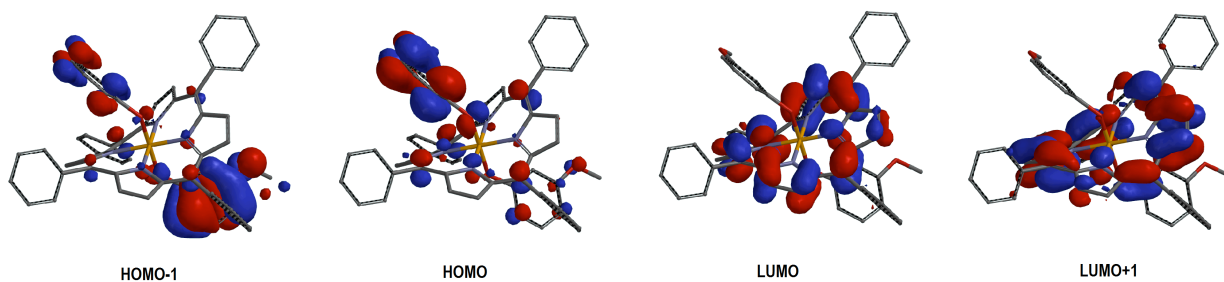


Figure S38 Calculated molecular orbitals of **4a**.

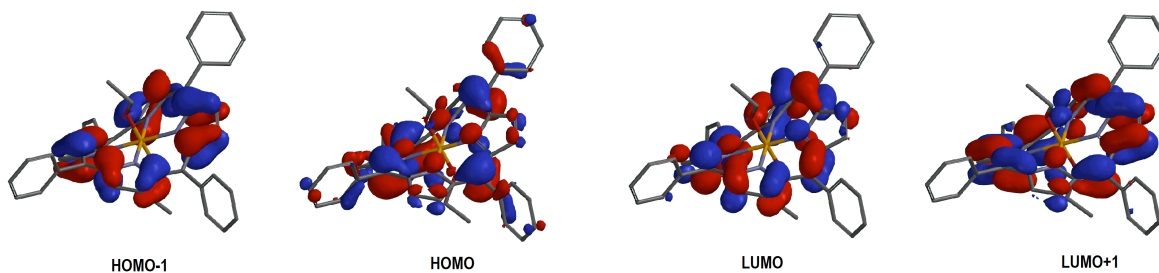


Figure S39 Calculated molecular orbitals of **5a**.

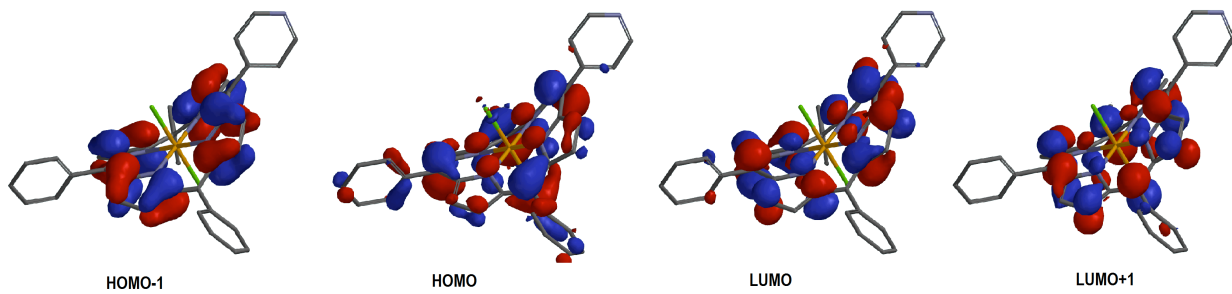


Figure S40 Calculated molecular orbitals of **2b**.

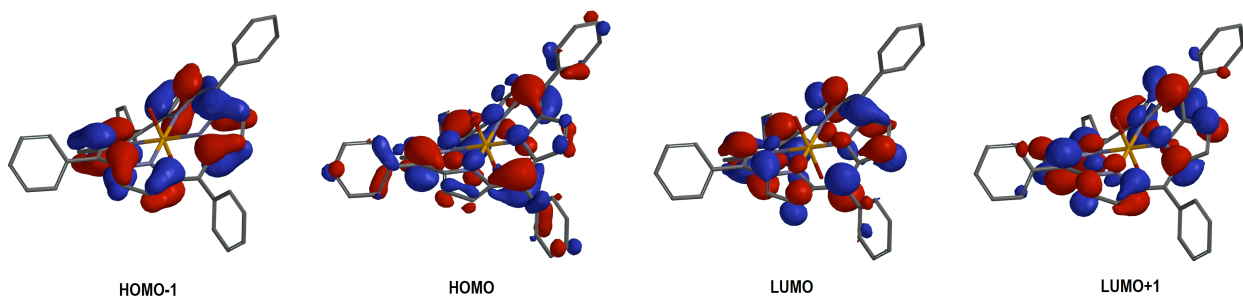


Figure S41 Calculated molecular orbitals of **3b**.

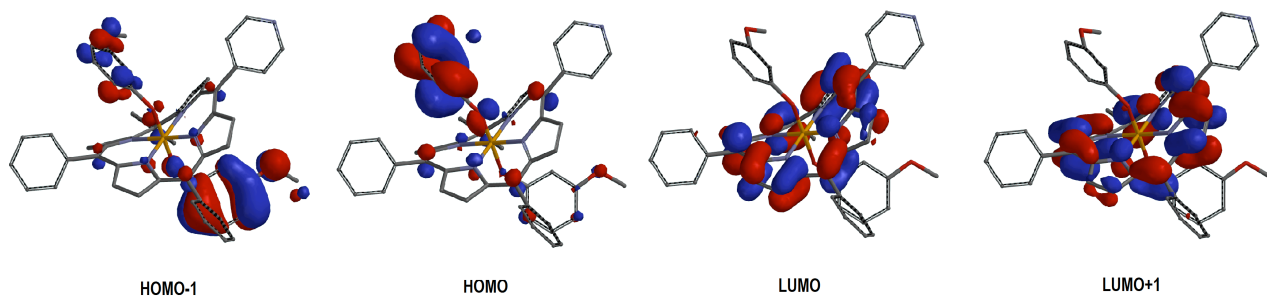


Figure S42 Calculated molecular orbitals of **4b**.

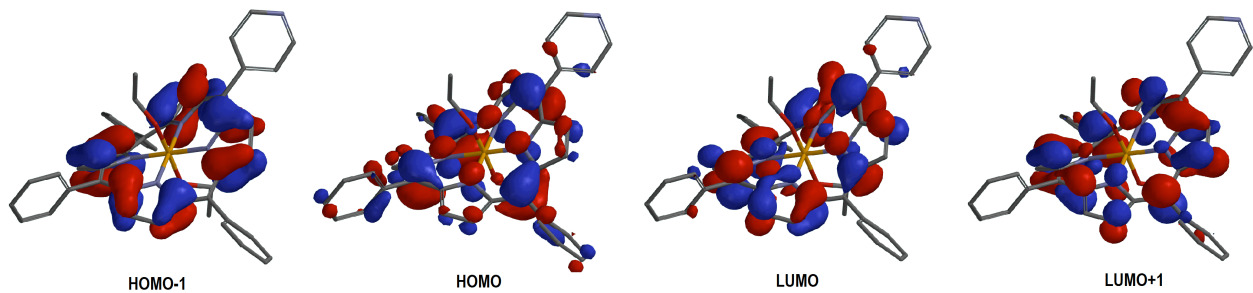


Figure S43 Calculated molecular orbitals of **5b**.

References

- 1 M. T. Barton, N. M. Rowley, P. R. Ashton, C. J. Jones, N. Spencer, M. S. Tolleya and L. J. Yellowleesb, *New J. Chem.*, 2000, **24**, 555–560.
- 2 C. J. Carrano and M. Tsutsui, *J. Coord. Chem.*, 1977, **7**, 79–83.
- 3 J. P. Strachan, S. Gentemann, J. Seth, W. A. Kalsbeck, J. S. Lindsey, D. Holten and D. F. Bocian, *J. Am. Chem. Soc.*, 1997, **119**, 11191–11201.
- 4 R. Schmidt, K. Seikel and H.-D. Brauer, *J. Phys. Chem.*, 1989, **93**, 4507–4511.
- 5 J. Davila and A. Harriman, *Photochem. Photobiol.*, 1990, **51**, 9–19.
- 6 K. Shirono, T. Morimatsu and F. Takemura, *J. Chem. Eng. Data*, 2008, **53**, 1867–1871.
- 7 D. Lala, J. F. Rabek and B. Ranby, *Eur. Polym. J.*, 1980, **16**, 735–744.
- 8 E. N. Golubeva, E. M. Zubanova, M. Y. Melnikov, F. E. Gostev, I. V. Shelaev and V. A. Nadochenko, *Dalt. Trans.*, 2014, **43**, 17820–17827.